Fossil Record 29 (1) 2026, 87–113 | DOI 10.3897/fr.29.178152

PENSOFT

MUSEUM FÜR NATURKUNDE BERLIN

A new dinosaur species from Korea and its implications for early-diverging neornithischian diversity

Jongyun Jung[1,2], Minguk Kim[2], Hyemin Jo[3,4], Julia A. Clarke[1]

1 *Department of Earth and Planetary Sciences, Jackson School of Geosciences, The University of Texas at Austin, Austin, USA*
2 *Korea Dinosaur Research Center, Chonnam National University, Gwangju, Republic of Korea*
3 *Gwangju National Science Museum, Gwangju, Republic of Korea*
4 *Department of Geological and Environmental Sciences, Chonnam National University, Gwangju, Republic of Korea*

https://zoobank.org/83804EE9-28F5-42B8-AAA2-787D2BC337C6

Corresponding authors: Jongyun Jung (jongyunjung1991@gmail.com); Julia A. Clarke (julia_clarke@jsg.utexas.edu)

Academic editor: F. Witzmann ♦ **Received** 14 November 2025 ♦ **Accepted** 22 February 2026 ♦ **Published** 19 March 2026

Abstract

The Korean dinosaur fossil record is exceptionally rich in trackways and eggs, yet skeletal remains are exceedingly rare. Two species have been described based on postcranial elements, and a taxon known from cranial materials has not yet been reported. Here, we report a new early-diverging neornithischian species, known from a small, partially articulated skeleton comprising cranial and postcranial elements as well as gastroliths. The specimen is from the mid-Cretaceous Ilseongsan Formation of Aphae Island (Aphaedo). X-ray micro-computed tomography (micro-CT) revealed the anatomy of the new species, including the first studied cranial remains of a dinosaur from Korea. The size and anatomical features of the specimen, along with histological analysis, indicate that it is not a fully grown individual, probably 0–2 years old. Gastroliths are present, with morphologies and a relative mass proposed to be consistent with a more omnivorous diet. Phylogenetic analyses recover the new species, *Doolysaurus huhmini* **gen. et sp. nov.**, as a thescelosaurid. The recovery of *Doolysaurus* with most other Asian thescelosaurids near the base of this clade provides further evidence for its origin and early biogeography. The new discovery suggests that other small dinosaur fossils may be found at Aphaedo or at sites with similar taphonomic conditions in Korea; *Doolysaurus* is consistent with richer dinosaurian diversity in the Cretaceous of Korea than is represented in its rich trace fossil record.

Key Words

Aphaedo, *Doolysaurus huhmini*, mid-Cretaceous, Neornithischia, Thescelosauridae, Shinan

Introduction

The dinosaur skeletal fossil record in Korea has long been limited in both abundance and completeness. Chang et al. (1982) reported the first bone from a dinosaur, a find that was followed by a limited number of similarly fragmentary postcranial elements (Choi and Lee 2017; Kim and Huh 2018). Although several taxa, such as *Ultrasaurus tapriensis* (Chang et al. 1982; Kim 1983) and *Pukyungosaurus milleniumi* (Dong et al. 2001), were erected, these are now regarded as nomina dubia due to the absence of unique autapomorphies and the lack of sufficient morphological information (Lee and Yang 1997; Park 2016). Additional reports of isolated and fragmentary bones, such as a theropod dorsal rib and a neornithischian pedal phalanx, have also been documented (Lee 2008; Lee et al. 2024), but their phylogenetic affinities remain uncertain (Choi and Lee 2017). To date, only two dinosaur taxa from Korea are known from Late Cretaceous partial postcranial skeletons, the basal ceratopsian *Koreaceratops hwaseongensis* (Lee et al. 2011) and the early-diverging neornithischian *Koreanosaurus boseongensis* (Huh et al. 2011) from the Seonso Conglomerate (81 Ma).

A new dinosaur skeleton was recovered from the Ilseongsan Formation, where it crops out on the shoreline

of Aphae Island (hereafter, Aphaedo; Fig. 1), Shinan, on the southwestern coast of the Republic of Korea. A newly discovered fossil site on the island samples stratigraphic units underlying those of the Aphaedaegyo Bridge section, where an exceptionally preserved nest of giant theropod eggs (*Macroelongatoolithus*) was discovered (Huh et al. 2014). Vertebrate skeletons, the *Macroelongatoolithus* nest, and other diverse types of dinosaur eggs were discovered in homogeneous, reddish-brown, fine-grained sandy mudstones interbedded with gray pyroclastic units. These homogeneous layers have paleosol profiles with calcareous nodules (Fig. 1B), in contrast to the coarser sandstones and conglomerates that overlie and underlie the fossil-bearing units.

The homogeneous sandy mudstones with paleosol profiles and calcareous nodules represent steady and relatively rapid sedimentation, indicating a distal floodplain environment (Kraus 1999; Kim et al. 2022). In addition, the sequence of stratified deposits containing fragments of bone and eggshell, with gravelly sandstone layers, is interpreted as crevasse-splay deposits. Comparable depositional settings have been reported from several egg fossil sites in Korea, including Boseong (Paik et al. 2004), Wi Island (Kim et al. 2022), and the upper Hasandong Formation (Paik 2000). Similarly, the Gaogou Formation in Henan Province, China, where eggs such as *Macroelongatoolithus*, *Dendroolithus*, and various other dinosaur eggs have been documented, has been interpreted as a river floodplain deposit preserved through overflow events (Liang et al. 2009), closely resembling the depositional context of the Aphaedo site.

The Ilseongsan Formation conformably overlies the Injiri Formation and is overlain by the Dalido Formation; the Dalido Formation is unconformably overlain by a tuffaceous unit, the Maewolli Tuff (Kim et al. 2014). The age of the Cretaceous strata on Aphaedo Island, including the Ilseongsan Formation, has been a subject of some controversy. Rhee et al. (2012) first estimated the age of the Ilseongsan Formation as 77–83 Ma based on K-Ar dating of volcanic pebbles from conglomerate units of this formation and samples from an overlying tuff. However, Kim et al. (2014) re-dated this tuff, now named the Maewolli Tuff, to 97.55 ± 0.62 Ma using U-Pb SHRIMP zircon analysis, indicating that the Dalido Formation as well as the underlying Injiri and Ilseongsan formations are significantly older. Choi et al. (2023) estimated the age of the Dalido and Ilseongsan formations as ranging from the Albian to the Cenomanian (~113–94 Ma) based on the affinities of ostracods from the Dalido Formation and the stratigraphic distribution of *Macroelongatoolithus* (Simon et al. 2018), the oldest global occurrence of which is Albian (Choi et al. 2023). Thus, given the broader agreement of vertebrate and invertebrate biostratigraphic data with the older estimated age for the Maewolli Tuff, we consider the Ilseongsan Formation to be mid-Cretaceous (Albian–early Cenomanian; ~113–97 Ma) in age.

Here, we describe a small, well-preserved skeleton including both cranial and postcranial elements, as well as associated gastroliths, utilizing X-ray micro-computed tomography (micro-CT). This specimen, recognized as the holotype of a new genus and species, *Doolysaurus huhmini* gen. et sp. nov. (Fig. 2), includes the first diagnostic cranial material of a dinosaur from Korea. Histological data were acquired to assess the ontogenetic status of the new individual. We then investigated the phylogenetic position and ecology of this new dinosaur. It contributes novel insights into the diversity of the Korean dinosaur fauna, which has previously been known primarily from ichnofossil and egg fossil records.

Materials and methods

Institutional abbreviations

IGM: Institute of Geology, Mongolian Academy of Sciences, Ulaan Baatar, Mongolia; **KDRC**: Korea Dinosaur Research Center, Chonnam National University, Gwangju, South Korea; **MWC**: Museum of Western Colorado, Grand Junction, Colorado; **NCSM**: North Carolina Museum of Natural Sciences, Raleigh, North Carolina; **YLSNHM**: Yingliang Stone Natural History Museum, Nan'an, China.

Micro-CT analysis

The specimen KDRC-SA-V001 was CT-scanned using the NSI Scanner at the University of Texas High-Resolution X-ray Computed Tomography Facility (UTCT). Three scans were performed on the whole block, cranial region, and hindlimbs with the following settings: 200 kV/0.27 mA, 1889 total slices, and a voxel size of 134.2 µm for the whole block; 200 kV/0.31 mA, 1856 total slices, and a voxel size of 60.9 µm for the cranial region; 210 kV/0.325 mA, 1863 total slices, and a voxel size of 93.4 µm for the hindlimb region. Segmentation of the skeleton was performed using Dragonfly 3D World (v. 2024.1). Osteological visualization was generated in orthographic view using Blender (v. 4.4.3). Comparative 3D models of *Koreanosaurus* (femur and tibia) were acquired using a 3D Scanner Solutionix Rexcan 4. The 3D models were uploaded to MorphoSource and are available to the public (https://www.morphosource.org/concern/biological_specimens/000821427).

Bone histology

A histological thin section of the femur of KDRC-SA-V001 was prepared and is reposited at the Korea Dinosaur Research Center, Chonnam National University. A single transverse section was acquired just above the fourth trochanter of the left femur. Microscopic photographs were captured under both plane- and cross-polarized light using a petrographic microscope NIKON LV100W POL, and thin-section images were captured with a NIKON Ds-FI3 digital camera.

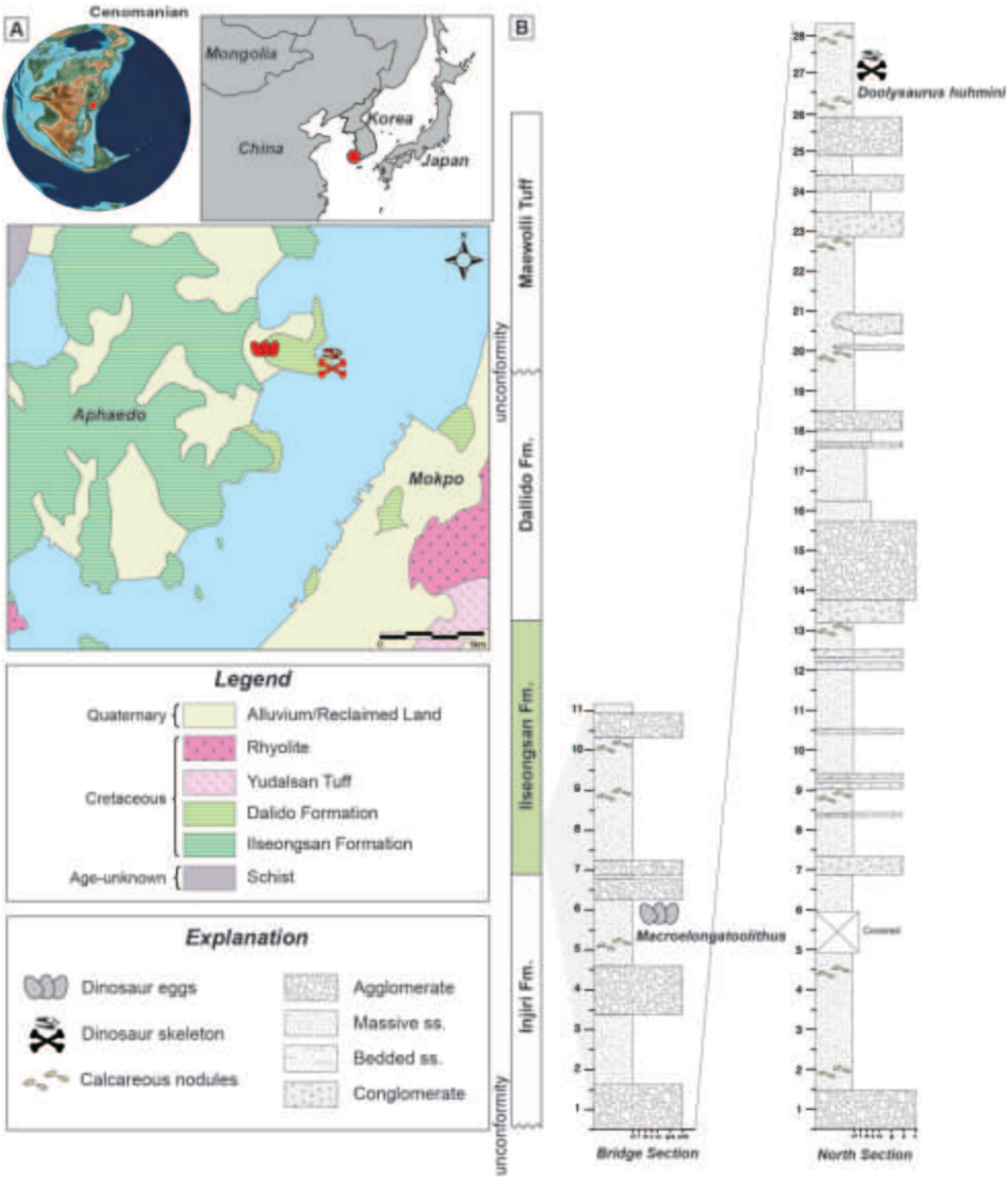

Figure 1. Geological and geographical setting of the Aphaedo site. **A.** The paleogeographic reconstruction corresponds to 100 Ma (Cenomanian) and a geological map of the Aphaedo site. The paleogeographic map is modified after Scotese (2021); **B.** Stratigraphic sections of the fossil-bearing sites.

Phylogenetic analyses

To determine the phylogenetic position of the new species, we employed the matrix of Fonseca et al. (2024). However, to test the sensitivity of the recovered phylogenetic position of the new species, we also ran supplemental analyses using the 300+ character dataset of Avrahami et al. (2024); analytical parameters are presented in the Suppl. materials 1–7. The Fonseca et al. (2024) matrix includes a broader sampling of ornithischian taxa (174) and a larger set of morphological characters (+900). This matrix also indicates ontogenetically variable characteristics that may appear in ornithischians, and these were examined together. In this dataset, we newly scored the taxon *Fona herzogae* (Avrahami et al. 2024). In addition, scorings for *Koreanosaurus boseongensis* (Huh et al. 2011) and *Jeholosaurus shangyuanensis* (Xu et al.,

2000) were revised in both datasets based on reexamination of *K. boseongensis* specimens KDRC-BB1, -BB2, and -BB3, as well as new scoring information from the micro-CT skull data of *J. shangyuanensis* specimen YLSNHM 01942 (Bertozzo et al. 2025). The revised scoring information of *K. boseongensis* and *J. shangyuanensis* is provided in the Suppl. materials 1–7. In both datasets, characters ordered by the original authors were also ordered here. All characters were equally weighted.

Parsimony analyses were performed using TNT v. 1.6 (Goloboff and Morales 2023) with equally weighted characters. A total of 200,000 of the most parsimonious trees were retained in memory. The heuristic search employed the "New Technology Search" with the default parameters for sectoral search, drift, and tree-fusing, with 100 replications. The "Find minimum length" criterion was set to 100, specifying the number of search hits required to confirm that the minimum tree length had been reached and thereby terminating the search once this threshold was satisfied. The replication parameter was set within the range reported by Fonseca et al. (2024), with the number of replications varying from 20 to 100. To ensure methodological consistency, we adopted the same setting as in Fonseca et al. (2024), corresponding to the upper bound of their reported range. The trees recovered from this search were subsequently subjected to an additional round of Tree Bisection and Reconnection (TBR) using the "Traditional Search." *Euparkeria capensis* was set as the outgroup. All TNT input files, search parameters, and scripts are available in the Suppl. materials 1–7.

We also conducted Bayesian tip-dated analyses using MrBayes v. 3.2.7 (Ronquist et al. 2012). Morphological evolution was modeled under the Mkv model (Lewis 2001) with a gamma-distributed rate variation across characters. An independent gamma rates (IGR) relaxed-clock model was employed. Divergence times were estimated under the Fossilized Birth-Death (FBD) model. The sampling proportion was set to 0.0002. Tip ages were constrained following the mean of the minimum and maximum ages from the Paleobiology Database (PBDB; http://paleobiodb.org), with the tip age of *Doolysaurus huhmini* fixed at 103.45 Ma, the midpoint of the Albian and Cenomanian. The tree age prior followed an offset exponential distribution (minimum 244 Ma, mean 260 Ma), consistent with the stratigraphic record. The Markov chain Monte Carlo (MCMC) analysis was run for 10,000,000 generations, sampling every 2000 generations, with the first 25% of samples discarded as burn-in. Tree data were visualized using FigTree (v. 1.4.4) and Adobe Illustrator 2025. All NEXUS files and results are available in the Suppl. materials 1–7. Below, in the diagnosis, we discuss the results of the analyses of the Fonseca et al. (2024) dataset. Major results from sensitivity analyses utilizing the Avrahami et al. (2024) dataset are reported in the text and are also detailed in the figures in the Suppl. materials 1–7.

Systematic paleontology

Dinosauria Owen, 1842
Ornithischia Seeley, 1887
Neornithischia Cooper, 1985
Thescelosauridae Sternberg, 1937

***Doolysaurus* gen. nov.**
https://zoobank.org/86C724BC-2A9E-47EB-A502-898E4FBAC0BD

Type species. *Doolysaurus huhmini* sp. nov.

***Doolysaurus huhmini* sp. nov.**
https://zoobank.org/895C6714-B565-4100-BE78-0F6AFE1537FE

Holotype. KDRC-SA-V001, is an associated partial skeleton preserved three-dimensionally in two contiguous blocks within a reddish, homogeneous, sandy mudstone (Figs 2–13) consisting of a partial cranial skeleton including dentary, maxilla, maxillary and dentary teeth, quadrate, supraoccipital, fused exoccipital/opisthotic, basioccipital, basisphenoid, and postcranial elements including dorsal vertebrae, ribs, tibia, fibula, femur, metatarsals, and pedal phalanges (Figs 2–13). While the cranial and axial elements are disarticulated, the hindlimb elements are well articulated. Within the block, the skeletal components are preserved in a sub-planar arrangement (Fig. 2). The specimen, which contains a small cluster of gastroliths, was discovered by one of the authors, H.J., and is housed at the Korea Dinosaur Research Center, Chonnam National University, Gwangju, Republic of Korea. KDRC-SA-V001 is considered a juvenile individual based on its small size, unfused cranial elements and vertebrae, and histological assessment of a section of the femoral diaphysis (see discussion below).

Type locality and horizon. Ilseongsan Formation (Albian – Cenomanian) cropping out on the southeastern coast of Aphae Island (Aphaedo), Shinan, Republic of Korea.

Etymology. The generic name *Doolysaurus* honors "Dooly the Little Dinosaur," an iconic Korean cartoon baby dinosaur character created by Soo-Jung Kim in 1983; saurus is from the Greek σαῦρος (sauros), meaning "lizard." The specific name, *huhmini*, honors Professor Dr. Min Huh, a paleontologist who conducted research on a theropod fossil nest from the Aphaedo site, in recognition of his outstanding contributions to the study of dinosaurs in Korea over the past 30 years.

Nomenclatural acts. This publication and the nomenclatural acts in the contents are registered in Zoobank. The publication is registered under LSID [urn:lsid:zoobank.org:pub:83804EE9-28F5-42B8-AAA2-787D2BC337C6], the new genus *Doolysaurus* under LSID [urn:lsid:zoobank.org:act:86C724BC-2A9E-47EB-A502-898E4FBAC0BD], and the new species *Doolysaurus huhmini* is under LSID [urn:lsid:zoobank.org:act:895C6714-B565-4100-BE78-0F6AFE1537FE].

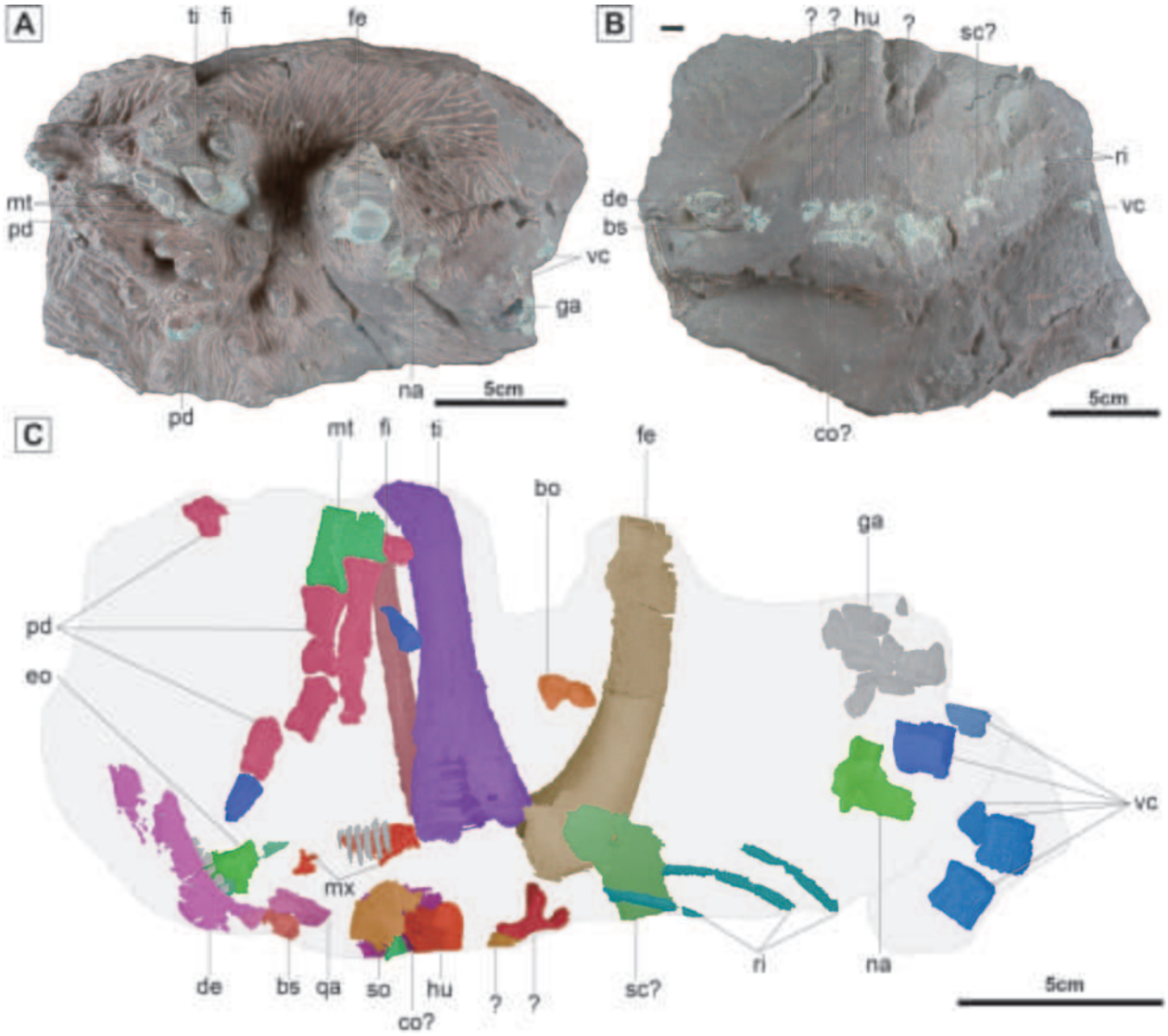

Figure 2. Block KDRC-SA-V001 bearing the holotype of *Doolysaurus huhmini* gen. et sp. nov. **A, B.** Photographs of KDRC-SA-V001; **C.** Digitally rendered models of the bones of KDRC-SA-V001 from CT scan data. Abbreviations: bo: basioccipital; bs: basisphenoid; co: coracoid; de: dentary; eo: exoccipital-opisthotic; fe: femur; fi: fibula; ga: gastrolith; hu: humerus; mt: metatarsal; na: neural arch; pd: pedal digits; qa: quadrate; ri: rib; sc: scapula; so: supraoccipital; ti: tibia; vc: vertebral centrum.

Diagnosis. *Doolysaurus huhmini* is a small-bodied, early-diverging neornithischian dinosaur with the following unique combination of features recovered from analysis of the Fonseca et al. (2024) dataset, including one optimized autapomorphy (*): (1) the lateral condyle of the quadrate is larger than the medial condyle (shared with *Orodromeus* and *Haya*) (ch.196:2); (2) Exoccipital, relative positions of the exits of the hypoglossal nerve (XII) combined into a single exit (shared with *Jeholosaurus*) (ch. 254:2); (3) Basioccipital, contribution to the border of the foramen magnum more than 1/3 its basioccipital condyle size (shared with *Fona*) (ch. 261: 0); (4) the apex of the maxillary teeth is located posterior to the center (shared with *Zephyrosaurus*) (ch.431:1); (5) the neural spine's lateral expansion on the distal end of the dorsal vertebrae is absent (shared with *Orodromeus*) (ch.517:0); (6) Dorsal ribs, distal anteroposterior thickening present (shared with *Koreanosaurus*, *Thescelosaurus neglectus*, and *Th. garbanii*) (ch. 529: 1); (7) the maximum length of the distolateral femoral condyle as a percentage of its distal width is between 50% and 40% (shared with *Koreanosaurus*, *Orodromeus*, and *Oryctodromeus*) (ch.831:1); (8*) the lateromedial widths of the *crista tibiofibularis* and the medial condyle of the distal femur are roughly equal near the base (ch.833:0); (9) the cross-section of the fibular shaft is D-shaped (shared with *Albertadromeus*, *Koreanosaurus*, *Orodromeus*, *Oryctodromeus*, *Zephyrosaurus*, and *Fona*) (ch.855:1); (10) extensor pits are present on the distal ends of the proximal phalanges of pedal digits II–IV (shared with *Changmiania*, *Oryctodromeus*, and *Changchunsaurus*) (ch.914:1). Diagnosis of the genus is as for the species.

Differential diagnosis. *Doolysaurus* is differentiated from the two other Korean ornithischian species insofar as preserved elements can be compared. Direct comparison between *Doolysaurus* and *Koreaceratops* is not feasible

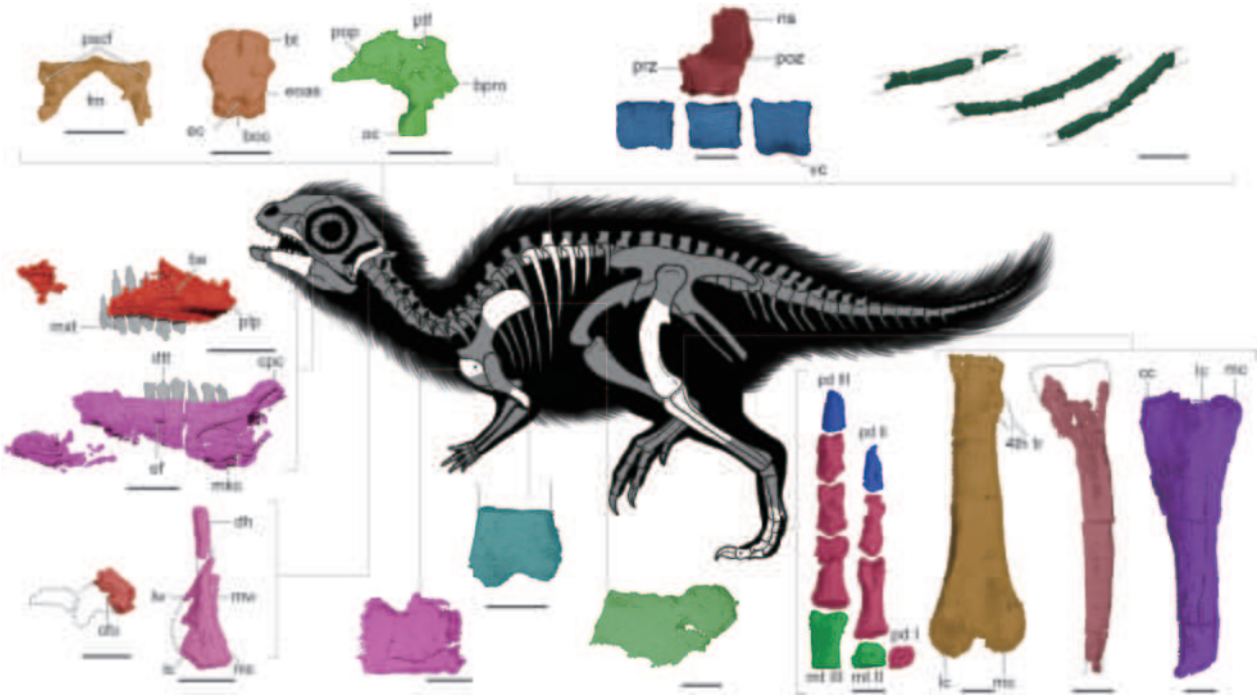

Figure 3. Skeletal anatomy of *Doolysaurus huhmini* gen. et sp. nov. All scale bars are 10 mm. Artwork by Janet Cañamar. Abbreviations: 4th tr: fourth trochanter; be: buccal emargination; boc: basioccipital condyle; bpro: boss for articulation with proatlas; bt: basal tubera; cc: cnemial condyle; cfo: carotid aorta foramen; cpc: coronoid process; dh: dorsal head; dtt: dentary tooth; ec: endocranial cavity; eoas: exoccipital articular surface; fm: foramen magnum; lc: lateral condyle; lw: lateral wing; mc: medial condyle; mkc: Meckelian canal; mt: metatarsal; mw: medial wing; mxt: maxillary tooth; ns: neural spine; oc: occipital condyle; pd: pedal digit; plp: posterolateral process; pop: paroccipital process; poz: postzygapophysis; prz: prezygapophyses; pscf: posterior semicircular canal foramen; ptf: posttemporal foramen.

because *Koreaceratops* preserves only a limited set of postcranial characters (Lee et al. 2011). Nevertheless, *Doolysaurus* can be distinguished from basal ceratopsians by cranial features including the presence of a fossa at the base of the posterior pterygoid wing on the quadrate (Ch. 195:1); absence of a nuchal crest on the supraoccipital (Ch. 245:0); pendent, ventrally extending distal ends of the paroccipital processes (Ch. 250:1); and subtriangular unworn non-caniniform maxillary crowns (Ch. 428:0). *Koreanosaurus boseongensis* (Huh et al. 2011) was discovered from the significantly younger Seonso Conglomerate (Santonian–Campanian) (Kim et al. 2008). However, specimens of the two taxa have limited anatomical overlap. Holotype and referred specimens of *Koreanosaurus* preserved the forelimbs, part of the axial skeleton, and the hindlimb, excluding the pes. Nevertheless, both specimens include the femur, tibia, fibula, and dorsal vertebrae.

Comparing shared elements and considering previously documented ontogenetic variation in neornithischians (e.g., Weishampel et al. 2003; Poole 2023; Pintore et al. 2025), we discuss notable differences both with *Koreanosaurus* and other taxa. Although both *Doolysaurus* and *Koreanosaurus* lack an anterior inner condyle groove on the femur (Ch. 826:0), the morphology of the anterior margin differs markedly between the two taxa (Fig. 4). In *Koreanosaurus*, the anterior margin of the distal femur is distinctly flat and meets the similarly flattened medial margin at a defined angle (Fig. 4A). In contrast, *Doolysaurus* exhibits a rounded anterior margin that transitions smoothly into the flat medial surface without a distinct angular boundary, similar to *Haya* (Makovicky et al. 2011; Barta and Norell 2021) (Fig. 4B). On the distal femur, the medial condyle of *Doolysaurus* is symmetrical (Fig. 4B), resembling the condition in *Haya* (Makovicky et al. 2011; Barta and Norell 2021) and *Thescelosaurus assiniboiensis* (Brown et al. 2011) (Fig. 4C). By contrast, *Koreanosaurus* exhibits an asymmetrical medial condyle (Fig. 4A), a condition similar to that observed in *Jeholosaurus* (Han et al. 2012) and *Parksosaurus* (Sues et al. 2023) (Fig. 4C). In addition, the femoral shaft of *Koreanosaurus* appears slightly more bowed than that of *Doolysaurus* (Ch. 781:0) (Fig. 4A, B). However, this difference may reflect ontogenetic variation. Poole (2023) reported that in iguanodontians such as *Tenontosaurus*, *Zalmoxes*, and *Camptosaurus*, juvenile individuals tend to exhibit a bowed femur, which becomes straighter in adults (Weishampel et al. 2003). Conversely, *Dryosaurus* shows the opposite trend (Poole 2023).

The proximal tibia of *Doolysaurus* exhibits a sharply defined and prominent lateral condyle, in contrast to the more gently rounded condyle observed in *Koreanosaurus* (Huh et al. 2011) (Fig. 5). This pronounced lateral condyle margin in *Doolysaurus* closely resembles that of *Albertadromeus* (Brown et al. 2013), in contrast to *Parksosaurus* (Sues et al. 2023), *Thescelosaurus assiniboiensis* (Brown et al. 2011), and *Orodromeus* (Scheetz

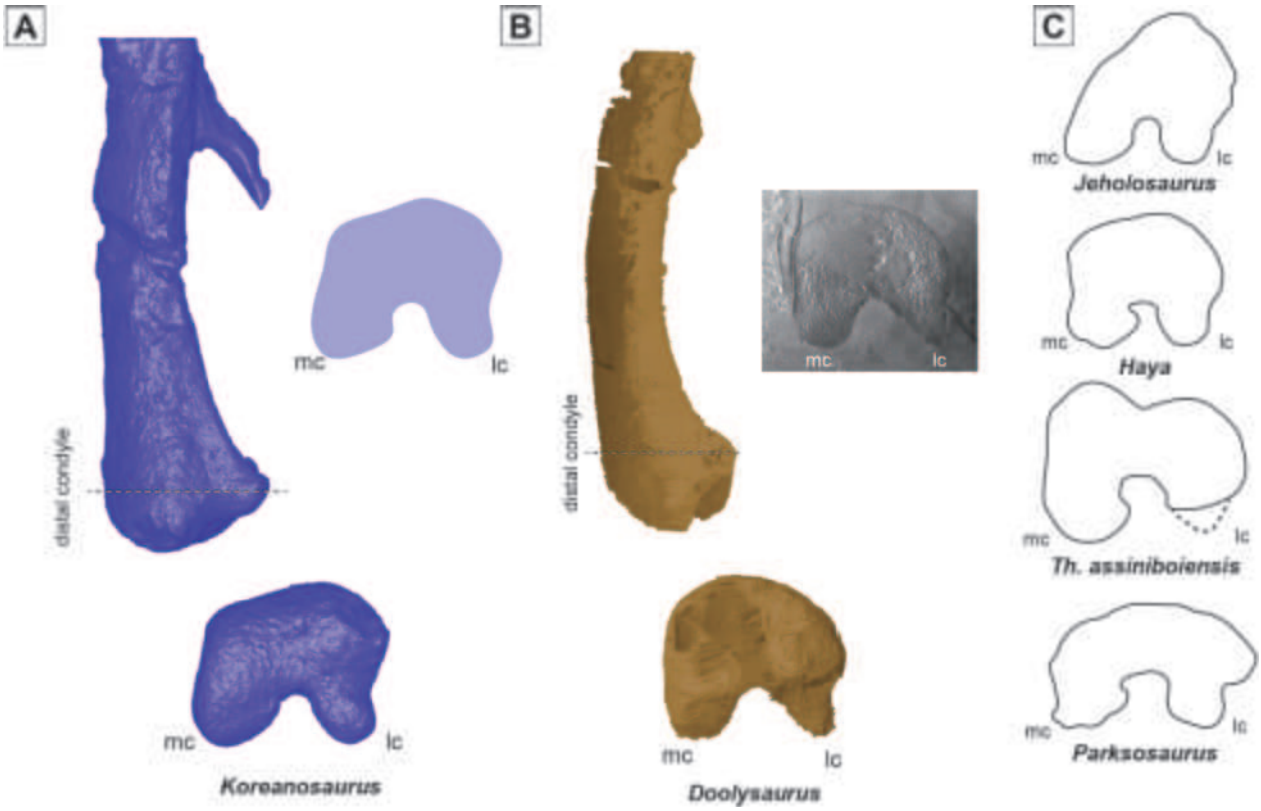

Figure 4. Comparison of the distal femoral morphology in early-diverging neornithischians. **A.** Distal femur of *Koreanosaurus boseongensis* in medial view (left), cross-sectional outline at the distal condyle (right), and ventral view of the distal condyle (bottom); **B.** Distal femur of *Doolysaurus huhmini* in medial view (left), cross-sectional CT-scanned image (right), and ventral view of the distal condyle (bottom); **C.** Comparative distal region of other early-diverging neornithischians, including *Jeholosaurus* (Han et al. 2012), *Haya* (Barta and Norell 2021), *Thescelosaurus assiniboiensis* (Brown et al. 2011), and *Parksosaurus* (Sues et al. 2023). All inset outlines are modified from images in Brown et al. (2011), Han et al. (2012), Barta and Norell (2021), and Sues et al. (2023) and were mirrored to facilitate comparison. All models and drawings are not to scale. Abbreviations: mc: medial condyle; lc: lateral condyle.

1999) (Fig. 5C). In addition, *Doolysaurus* lacks an accessory condyle on the proximal tibia (Ch. 844:0) (Fig. 5B), a condition shared with *Parksosaurus* (Sues et al. 2023) and *Thescelosaurus assiniboiensis* (Brown et al. 2011) (Fig. 5C). In contrast, *Koreanosaurus* possesses a well-developed accessory condyle in the same region (Huh et al. 2011) (Fig. 5A).

Doolysaurus differs from other Asian early-diverging neornithischian taxa in several cranial morphological characters. The apex of the maxillary crown is positioned posterior to the crown center (Ch. 431:0), whereas in *Jeholosaurus*, *Changchunsaurus*, *Haya*, and *Changmiania,* it is centrally placed. *Doolysaurus* lacks a prominent labial ridge on the maxillary crown (Ch. 434:0), unlike *Changmiania*, *Haya*, *Changchunsaurus*, and *Jeholosaurus*, which exhibit a triangular apicobasal ridge. In the tibia, *Doolysaurus* lacks an accessory condyle on the lateral proximal condyle (Ch. 844:0), a feature present in *Jeholosaurus*, *Changchunsaurus*, and *Haya*. *Doolysaurus* differs from *Yueosaurus* in possessing posteriorly projecting neural spines on the preserved dorsal vertebrae (Ch. 561:1), a round tibial midshaft (Ch. 846:1), and distinct extensor pits on the distal ends of pedal phalanges II–IV (Ch. 914:1).

Description. ***Skull.*** Most cranial elements are disarticulated and distributed in one area of the block (Fig. 6). The preserved two portions of the maxilla of KDRC-SA-V001 represent parts of the left element, and the more complete of these bears six maxillary teeth and nine alveoli (Fig. 6A). Because the posterior portion of the maxilla is incompletely preserved, the total number of maxillary teeth likely exceeded nine. No replacement teeth are present. The crowns are triangular in lingual and labial views, slightly asymmetrical, and laterally compressed, with a distinct constriction immediately above the root. Small denticles are developed along both the mesial and distal margins. The apices of the crowns, particularly in the posterior tooth row, are positioned posteriorly rather than centrally. A well-developed cingulum is present at the crown base, contrasting with the condition in *Parksosaurus* (Sues et al. 2023). Adjacent crowns are closely spaced without gaps, and the roots are straight in anterior and posterior views. The lateral maxillary surface exhibits a gentle dorsoventral concavity between the buccal ridge and the ventral margin of the external antorbital fenestra. A posterolateral process is present, resembling that of *Jeholosaurus* (Barrett and Han 2009; Bertozzo et al. 2025). Although the dorsal

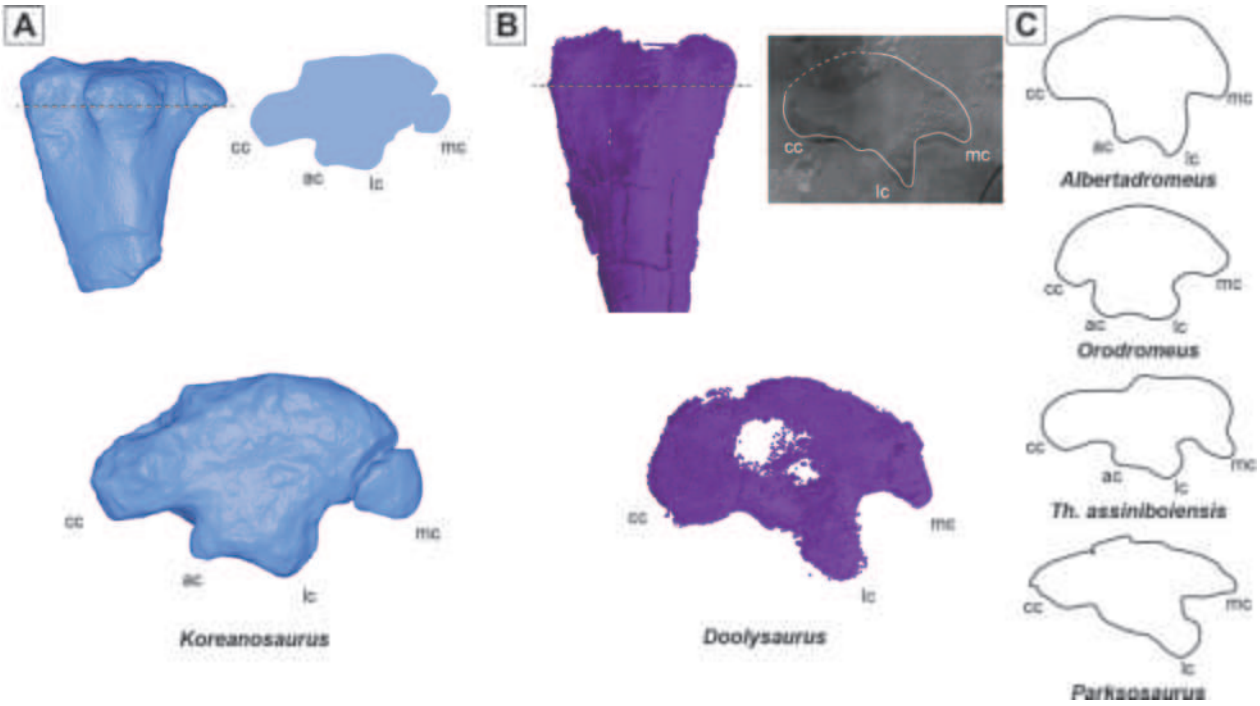

Figure 5. Comparison of the proximal tibial morphology in early-diverging neornithischians. **A.** Proximal tibia of *Koreanosaurus boseongensis* in lateral view (left), cross-sectional outline at the proximal condyle (right), and dorsal view of the proximal condyle (bottom); **B.** Proximal tibia of *Doolysaurus huhmini* in lateral view (left), cross-sectional CT-scanned image (right), and dorsal view of the proximal condyle (bottom); **C.** Comparative proximal region of other early-diverging neornithischians, including *Albertadromeus* (Brown et al. 2013), *Orodromeus* (Scheetz 1999), *Thescelosaurus assiniboiensis* (Brown et al. 2011), and *Parksosaurus* (Sues et al. 2023). All inset outlines are modified from images in Scheetz (1999), Brown et al. (2011), Brown et al. (2013), and Sues et al. (2023) and were mirrored to facilitate comparison. All models and drawings are not to scale. Abbreviations: ac: accessory condyle; cc: cnemial condyle; lc: lateral condyle; mc: medial condyle.

margin is damaged, the ventral edge is well preserved and displays a gentle slope.

The left dentary is preserved with 15 teeth and two replacement teeth, but the arrangement of alveoli suggests that the dentary could have accommodated at least 17 teeth (Fig. 6B). The cranial portion is broken and displaced. The dorsal margin remains relatively intact, whereas the ventral margin is damaged, obscuring whether it was initially straight or convex. In ventral view, the rostromedial edge curves slightly medially. The lateral surface is dorsoventrally convex and lacks the prominent ridge seen in *Changchunsaurus* (Jin et al. 2010) and the reduced ridge of *Changmiania* (Yang et al. 2020), instead resembling the condition in *Jeholosaurus* specimen YLSNHM 01942 (Bertozzo et al. 2025). Several foramina are present on the lateral surface, including a prominent elliptical foramen positioned within the buccal emargination, just posterior to the midlength of the dentary. The Meckelian canal is long and shallow, restricted to the ventral border of the medial surface of the anterior dentary. The coronoid process is straight and well developed, and the depth of the mandible at the coronoid is more than 140% of the depth of the mandible beneath the tooth row, resembling the condition in *Fona* (Avrahami et al. 2024), *Oryctodromeus* (Krumenacker et al. 2023), *Orodromeus* (Scheetz 1999), *Haya* (Makovicky et al. 2011; Barta and Norell 2021), *Changchunsaurus* (Jin et al. 2010), and *Jeholosaurus* (Barrett and Han 2009; Bertozzo et al. 2025). It is subtriangular in outline, posterodorsally oblique, and positioned posterior to the teeth, confluent with the axis of the tooth row.

An estimated tooth count of 17 dentary teeth would be similar to *Fona* (Avrahami et al. 2024), *Haya* (Makovicky et al. 2011; Barta and Norell 2021), *Changchunsaurus* (Jin et al. 2010), *Jeholosaurus* (Barrett and Han 2009; Bertozzo et al. 2025), and *Hypsilophodon* (Galton 1974), but differs from the higher count in *Thescelosaurus neglectus*, which possesses approximately 20 dentary teeth (Boyd 2014). This number also exceeds the 13–14 teeth reported for juvenile *Jeholosaurus* and more closely matches the 17 observed in mature individuals (Hu et al. 2024). *Dysalotosaurus* has fewer dentary teeth, with an estimated count of approximately 10 in juveniles and up to 13 in adults (Hübner and Rauhut 2010). Two replacement teeth are preserved, a condition also reported in *Jeholosaurus* (Hu et al. 2024; Bertozzo et al. 2025), *Thescelosaurus* (Morris 1976; Brown et al. 2011; Boyd 2014), *Haya* (Makovicky et al. 2011; Barta and Norell 2021), *Hypsilophodon* (Galton 1974), and *Parksosaurus* (Sues et al. 2023). The dentary crowns are triangular in lingual and labial aspects, distinctly constricted above the root, slightly asymmetrical, and laterally compressed. A pronounced primary ridge defines the apex, with denticles extending along both sides of the ridge.

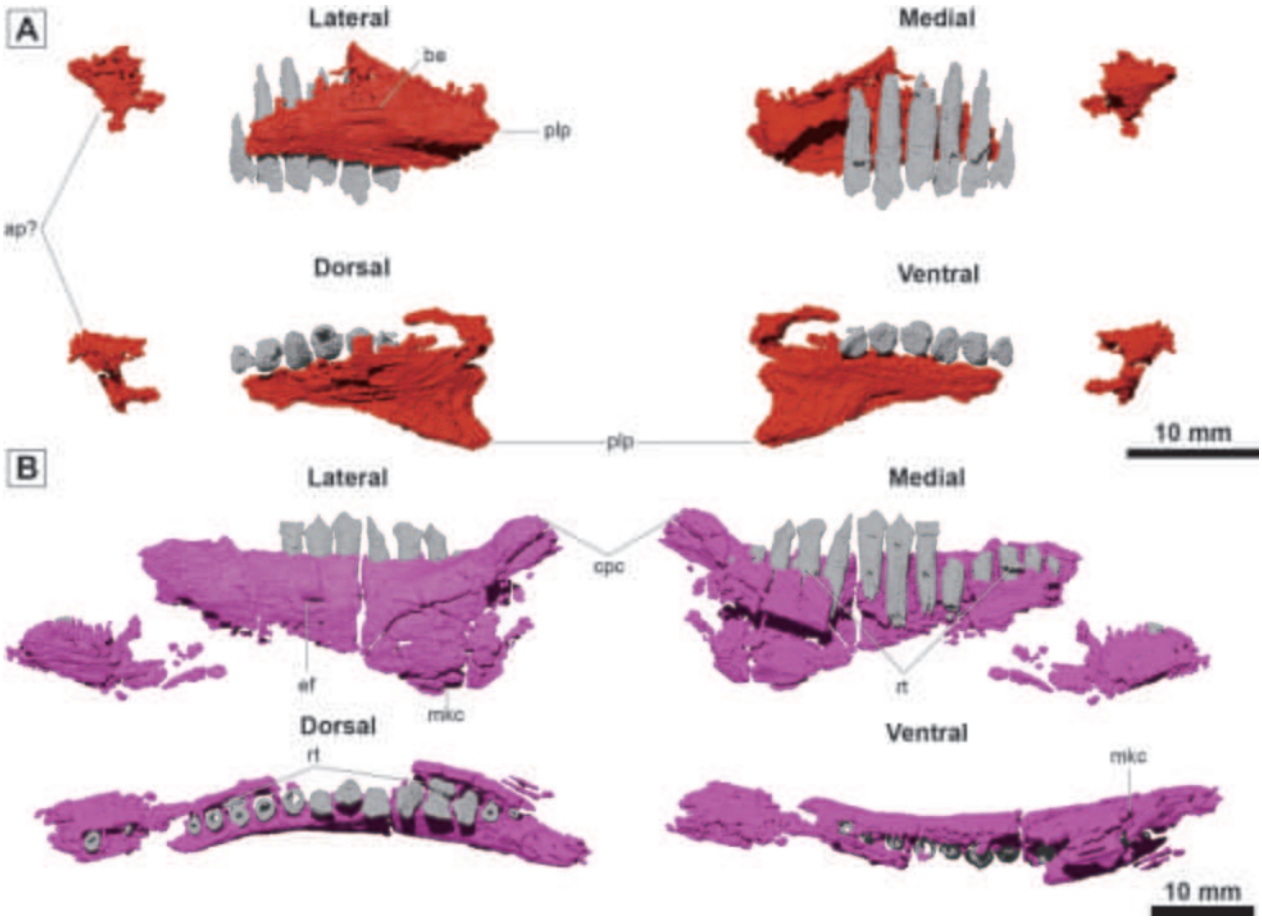

Figure 6. Left maxilla (**A**) and dentary (**B**) of the holotype specimen (KDRC-SA-V001). Abbreviations: ap: anterior process; be: buccal emargination; cpc: coronoid process; ef: elliptical foramen; mkc: Meckelian canal; plp: posterolateral process; rt: replacing tooth.

The cingulum is robust, and the roots are straight, unlike the more curved roots of *Parksosaurus* (Sues et al. 2023) and *Hypsilophodon* (Galton 1974). The anterior teeth are similar in morphology to more posterior teeth, resembling *Jeholosaurus* (Barrett and Han 2009; Bertozzo et al. 2025) but differing from *Thescelosaurus neglectus* (Boyd 2014), *Haya* (Makovicky et al. 2011; Barta and Norell 2021), and *Changchunsaurus* (Jin et al. 2010). The lingual surface of the crowns bears fewer than 10 secondary ridges. The primary ridge is markedly more prominent than the others, a condition shared with *Fona* (Avrahami et al. 2024), *Oryctodromeus* (Krumenacker et al. 2023), *Thescelosaurus neglectus* (Boyd 2014), *Haya* (Makovicky et al. 2011; Barta and Norell 2021), and *Changchunsaurus* (Jin et al. 2010), but distinct from *Zephyrosaurus* (Sues 1980), *Jeholosaurus* (Jin et al. 2010), and *Parksosaurus* (Sues et al. 2023). Wear facets appear developed along the entire tooth row, and the crowns exhibit mesiodistal expansion above the roots as well as weak labiolingual expansion, expressed as a distinct cingulum.

The left quadrate (Fig. 7) is dorsoventrally elongated with a blade-like appearance and a gently curved shaft, resembling the condition in other early-diverging neornithischians. The shaft is gently curved, with its ventral portion oriented vertically. The quadrate head is recurved posteriorly relative to the main axis, rounded in lateral view, and triangular in dorsal view. A pronounced ridge extends along the posteroventral side of the proximal end. The lateral wing is directed posteriorly with a transversely narrow anterior margin, whereas the medial (pterygoid) wing forms a large anteromedially directed fan of bone that arises below the dorsal head. The pterygoid ramus is not dorsoventrally narrow, and no prominent oval fossa is developed, although a distinct fossa occurs at the base of the posterior side of the pterygoid wing. No hamular process is present, as in *Changmiania* (Yang et al. 2020) and *Changchunsaurus* (Jin et al. 2010), but this character is variable in *Haya* (Barta and Norell 2021). A pit at the base of the jugal wing is absent. The lateral condyle is rounded and projects slightly more ventrally than the medial one, which is flatter. Based on the preserved part, the lateral condyle is estimated to be larger than the medial one, resembling the condition in *Orodromeus* (Scheetz 1999) and *Haya* (Barta and Norell 2021). In posterior view, the articular surface of the condyles is nearly horizontal.

Only the left fused exoccipital/opisthotic is preserved, and it is disarticulated from the other cranial elements (Fig. 8A). As in other early-diverging neornithischians, the left exoccipital/opisthotic of KDRC-SA-V001 is completely fused, with no visible suture between them

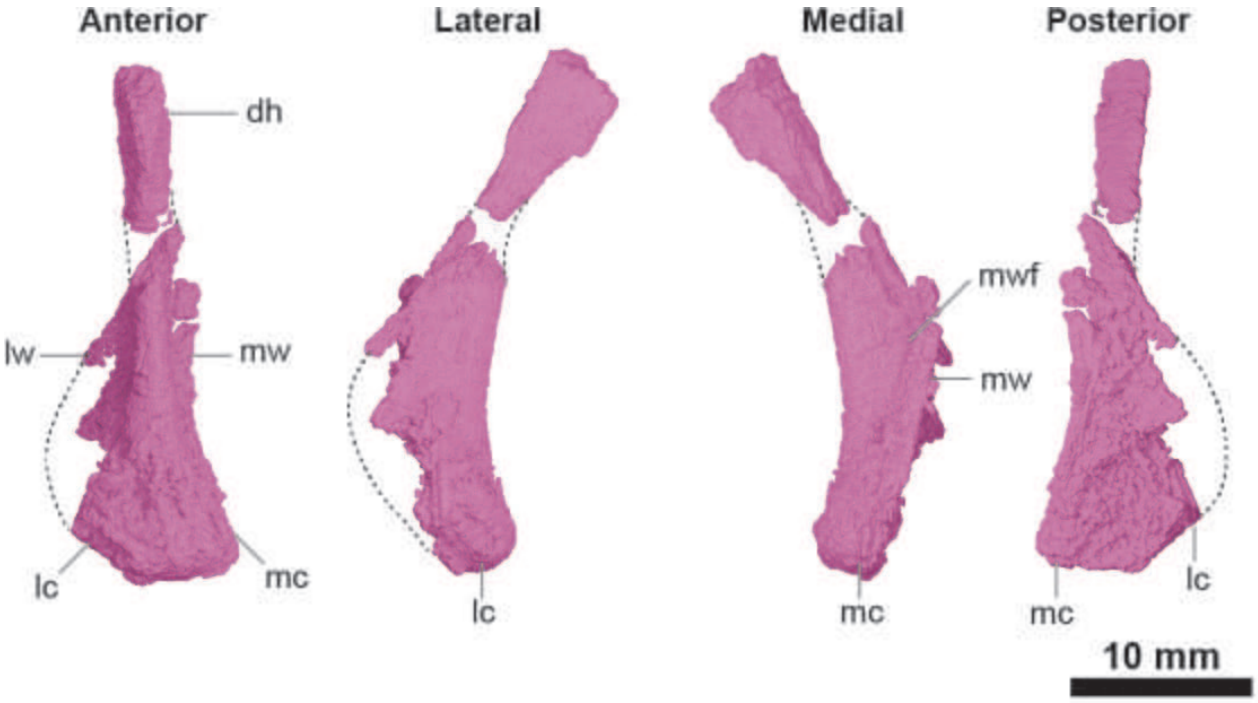

Figure 7. Left quadrate from the holotype specimen (KDRC-SA-V001). Abbreviations: dh: dorsal head; lc: lateral condyle; lw: lateral wing; mc: medial condyle; mw: medial wing; mwf: medial wing fossa.

(Norman 2004; Bertozzo et al. 2025). It is slightly twisted mediolaterally along its main axis, and a broad, trapezoidal paraoccipital process extends laterally, resembling the condition in *Jeholosaurus* (Bertozzo et al. 2025). This process is anteroposteriorly expanded rather than pendent, terminating in a subtriangular ventral tip that projects ventrally, similar to *Jeholosaurus* (Bertozzo et al. 2025), but differing from the morphology reported in *Haya* (Barta and Norell 2021). The posteroventral margin of the paraoccipital process bears no distinct scars for epaxial muscle attachment. On the anterolateral surface, a rod-like crista interfenestralis projects anteriorly, comparable to that in *Hypsilophodon* (Galton 1974) and *Jeholosaurus* (Bertozzo et al. 2025). The *recessus scalae tympani* is expressed as a wide, circular opening piercing the dorsal position of the exoccipital. A posteriorly projecting boss occurs on the dorsomedial corner of the posterior surface. The anterodorsal surface forms a complex articulation with the supraoccipital and is perforated by the foramen for the posterior semicircular canal. The posttemporal foramen is fully enclosed within the paraoccipital process, transmitting the *vena capitis dorsalis*, as in *Orodromeus* (Scheetz 1999), *Zephyrosaurus* (Sues 1980), *Haya* (Makovicky et al. 2011; Barta and Norell 2021), *Jeholosaurus* (Barrett and Han 2009; Bertozzo et al. 2025), and *Hypsilophodon* (Galton 1974). Two foramina pierce the ventral surface of the exoccipital: the larger posterior opening transmits cranial nerve XII, whereas the smaller, more anterior one likely corresponds to cranial nerve XI. Additionally, a single foramen on the medial surface also transmits branches of cranial nerve XII, indicating that the hypoglossal nerve exits were confluent into a single canal.

The supraoccipital is completely preserved (Fig. 8B). In posterior view, the posterodorsal surface is rhomboidal in outline and bears a subtle midline elevation instead of a prominent nuchal crest, a condition resembling that of *Fona* (Avrahami et al. 2024), *Thescelosaurus* (Brown et al. 2011; Boyd 2014), and *Haya* (Makovicky et al. 2011; Barta and Norell 2021). Two shallow depressions are developed laterally, parallel to the midline, as also noted in *Fona* (Avrahami et al. 2024) and *Thescelosaurus* (Boyd 2014). Unlike *Thescelosaurus neglectus* (Boyd 2014) and *T. assiniboiensis* (Brown et al. 2011), the dorsal surface lacks foramina. In dorsal view, the element is subtriangular. The posteroventral margin, which forms the dorsal border of the foramen magnum as in other early-diverging neornithischians, is distinctly concave. The articular surfaces for the prootic, laterosphenoid, and fused exoccipital/opisthotic are rough and perforated by small foramina.

The basioccipital is intact but is disarticulated from the other cranial elements (Fig. 8C). The occipital condyle is enlarged and vertically oriented, with considerable dorsoventral thickening and a slightly flattened articular surface. A wide U-shaped depression defines the ventral margin of the foramen magnum. The endocranial floor is slightly concave and bears a marked midline groove. This groove on the endocranial floor differs from that of other early-diverging neornithischians, which show either a midline ridge, such as *Thescelosaurus assiniboiensis* (Brown et al. 2011), *Zephyrosaurus* (Sues 1980), and *Jeholosaurus* (Bertozzo et al. 2025), or a flat endocranial surface, such as *Fona* (Avrahami et al. 2024), *Haya* (Makovicky et al. 2011; Barta and Norell 2021), *Oryctodromeus* (Krumenacker et al. 2023), and *Orodromeus* (Scheetz 1999). In ventral view, a well-developed keel divides

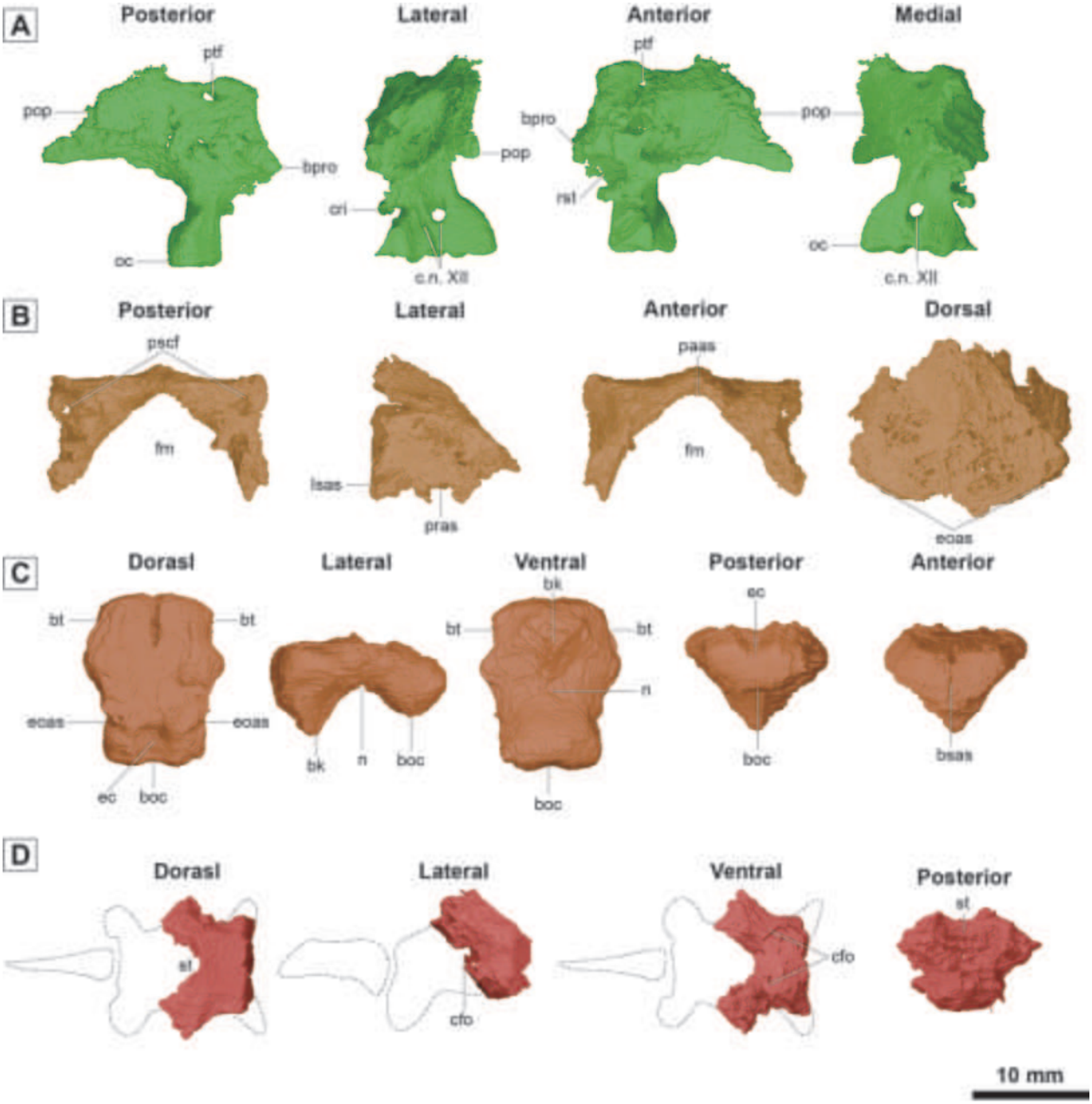

Figure 8. Basicranial region of the holotype specimen (KDRC-SA-V001): **A.** Left fused exoccipital/opisthotic; **B.** Supraoccipital; **C.** Basioccipital; and **D.** Basisphenoid. Abbreviations: bk: basioccipital keel; boc: basioccipital condyle; bpro: boss for articulation with proatlas; bass: basisphenoid articular surface; bt: basal tubera; cfo: carotid aorta foramen; cri: crista interfenestralis; ec: endocranial cavity; eoas: exoccipital articular surface; fm: foramen magnum; lsas: laterosphenoid articular surface; n: notch; oc: occipital condyle; paas: parietal articular surface; pop: paroccipital process; pras: prootic articular surface; pscf: posterior semicircular canal foramen; ptf: posttemporal foramen; rst: *recessus scalae tympani*; st: *sella turcica*.

the basal tubera, as seen in *Jeholosaurus* (Barrett and Han 2009; Bertozzo et al. 2025). The floor of the basioccipital is arched, resembling the condition in most early-diverging neornithischians. Although disarticulated, we estimate that the foramen magnum occupies more than 30% of the dorsal margin of the occipital condyle. This condition resembles that of *Fona* (Avrahami et al. 2024), *Oryctodromeus* (Krumenacker et al. 2023), *Th. assiniboiensis* (Brown et al. 2011), *Orodromeus* (Scheetz 1999), and *Haya* (Makovicky et al. 2011; Barta and Norell 2021), but differs from *Th. neglectus* (Boyd 2014) and *Th. garbanii* (Morris 1976).

Only the posterior portion of the basisphenoid is preserved at the margin of the block (Fig. 8D). The element is disarticulated, as are the other cranial components. The dorsoposterior surface is flat, bearing the posterior part of the *sella turcica*. The *sella turcica* is connected to two symmetrical grooves that extend along the ventral surface. The basipterygoid processes and the basioccipital articular surface are not preserved.

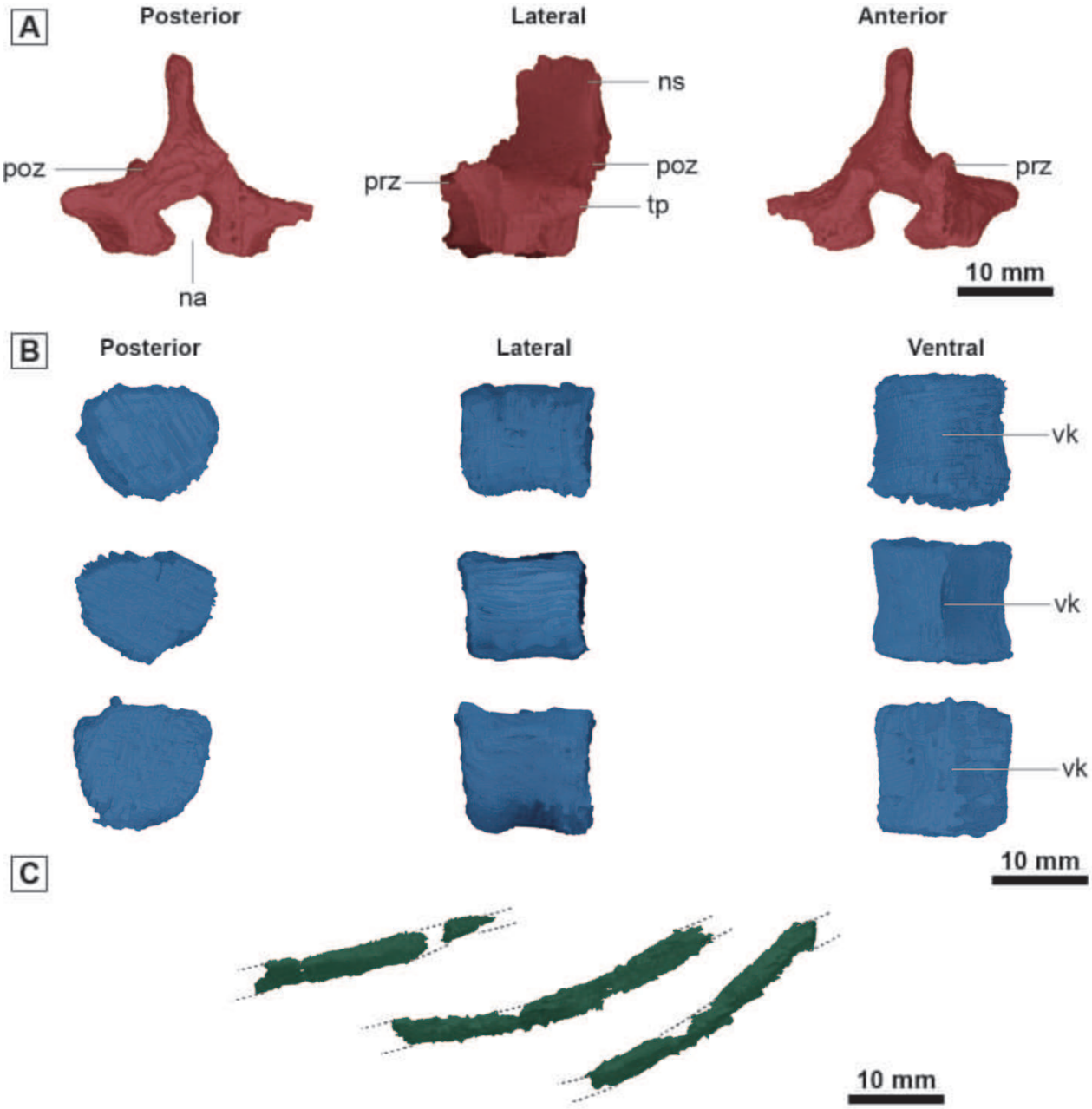

Figure 9. Dorsal vertebrae and ribs of the holotype specimen (KDRC-SA-V001): **A.** Dorsal neural arches; **B.** Vertebral centra; **C.** Dorsal ribs. Abbreviations: na: neural arch; ns: neural spine; poz: postzygapophysis; prz: prezygapophyses; tp: transverse process; vk: ventral keel.

Vertebrae and ribs. The dorsal vertebrae of KDRC-SA-V001 are represented by three complete isolated centra, two incomplete centra, and one complete neural arch (Fig. 9). All elements are unfused and disarticulated. The centra are amphicoelous (Fig. 9B). Their articular surfaces are subrounded to triangular in outline, with a flat dorsal surface and weak ventral keels. The keels are subdued, and considering the condition in other early-diverging neornithischians, in which the ventral keel diminishes posteriorly along the dorsal series, this feature suggests that the preserved centra likely belong to the anterior dorsal region. The floor of the neural canal is not pierced by any large, anteroposteriorly elongated foramen, resembling the condition in *Parksosaurus* (Sues et al. 2023) and *Thescelosaurus assiniboiensis* (Brown et al. 2011).

The preserved transverse processes are thin, cylindrical, and extend horizontally and approximately perpendicular in anterior view (Fig. 9A), as seen in *Changmiania* (Yang et al. 2020), *Albertadromeus* (Brown et al. 2013), *Koreanosaurus* (Huh et al. 2011), *Haya* (Makovicky et al. 2011; Barta and Norell 2021), *Changchunsaurus* (Jin et al. 2010), *Jeholosaurus* (Han et al. 2012), and *Parksosaurus* (Sues et al. 2023). The preserved prezygapophyses are short and process-like, whereas the postzygapophyses are damaged. The neural spines are positioned slightly posterior to the centra, a

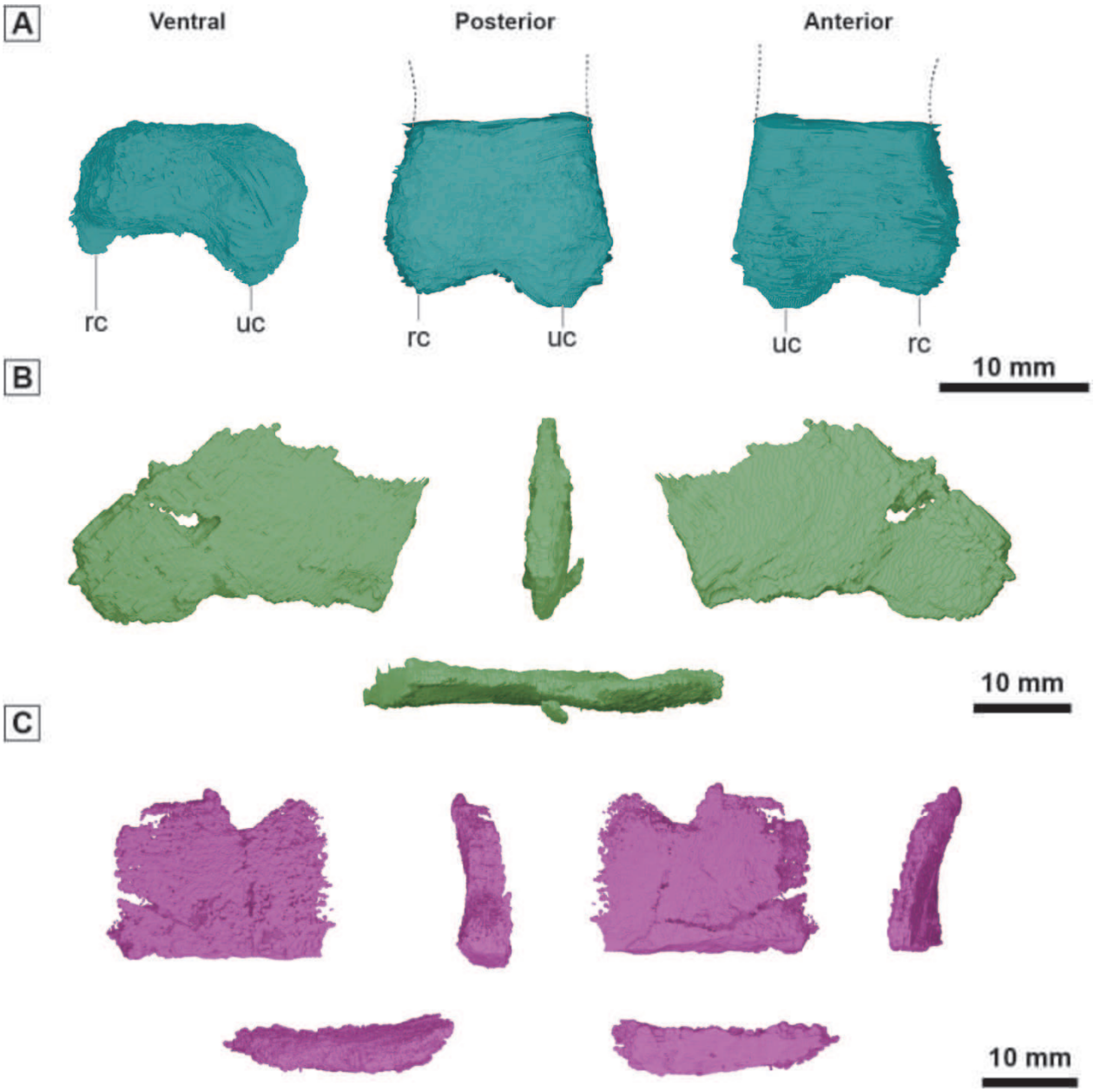

Figure 10. Pectoral girdle and forelimb elements of the holotype specimen (KDRC-SA-V001): **A.** Distal portion of the humerus; **B.** Possible fragment of the scapula; **C.** Possible fragment of the coracoid. Abbreviations: rc: radial condyle; uc: ulnar condyle.

morphology seen in *Koreanosaurus* (Huh et al. 2011), *Nevadadromeus* (Bonde et al. 2022), *Parksosaurus* (Sues et al. 2023), and *Thescelosaurus assiniboiensis* (Brown et al. 2011). The tips of the neural spines show no lateral expansion, as in *Orodromeus* (Scheetz 1999).

Three ribs are preserved in sequential arrangement, but their proximal ends are eroded at the specimen margin, making it difficult to determine their anatomical position (Fig. 9C). The rib shafts are strongly curved, and their cross sections are elliptical.

Forelimb. The forelimb elements of KDRC-SA-V001 are poorly preserved. Only the distal portion of the humerus (Fig. 10A) and possible fragments of the scapula (Fig. 10B) and coracoid (Fig. 10C) are exposed along the lower margin of the block. Most parts that would permit identification of diagnostic anatomical features are not preserved, obscuring detailed morphological assessment.

Hind limb. The distal left femur is preserved to the midshaft and remains roughly articulated with the tibia and fibula (Fig. 11). The shaft is slightly bowed anteriorly in lateral view and broadens distally. In cross-section, the midshaft is roughly circular to subelliptical, with the remnants of a posterolaterally projecting fourth trochanter. The fourth trochanter is prominent, but its distal end is damaged, making it difficult to confirm whether it has a pendant morphology similar to that of other early-diverging neornithischians. At the base of the fourth trochanter, an elongated shallow depression is present on the medial surface of the shaft, representing the insertion scar of the *m. caudofemoralis longus*.

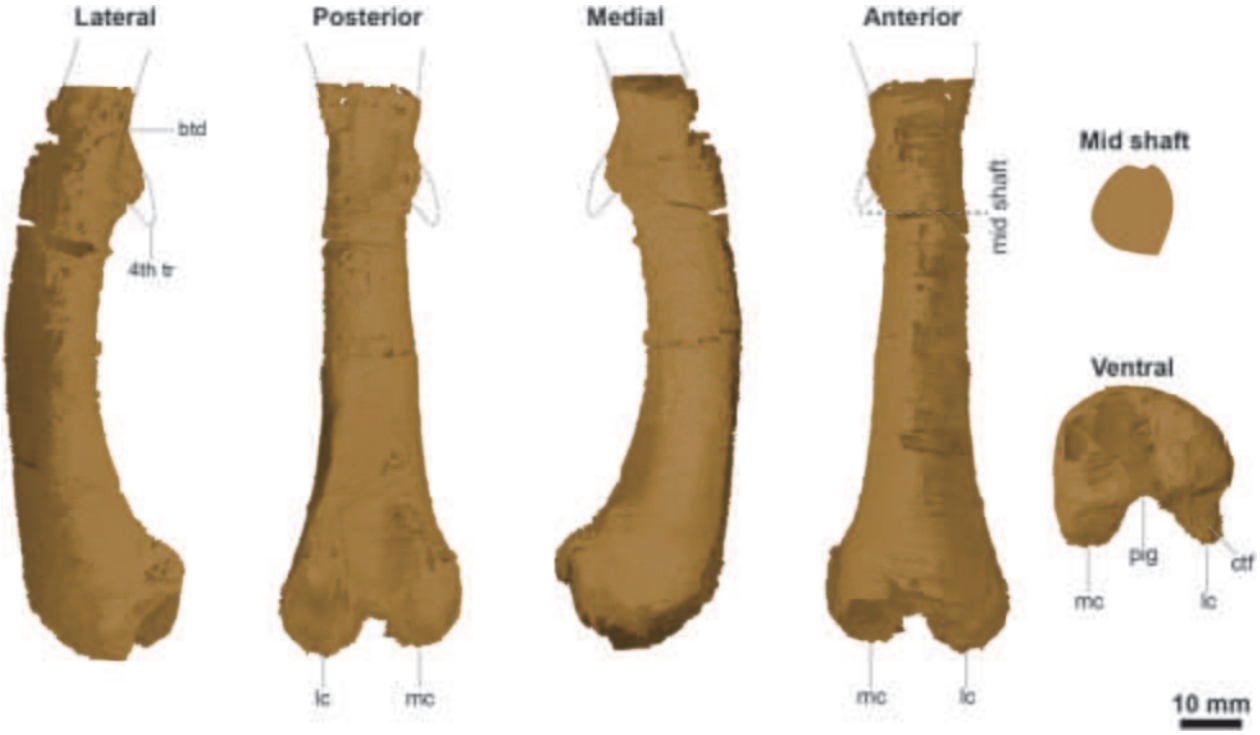

Figure 11. Left femur of the holotype specimen (KDRC-SA-V001). Abbreviations: 4th tr: fourth trochanter; btd: basitrochanteric depression; lc: lateral condyle; mc: medial condyle; pig: posterior intercondylar groove.

The distal end of the femur is expanded anteroposteriorly, with the medial and lateral condyles separated by a fully open posterior (flexor) intercondylar groove. The medial condyle is larger than the lateral condyle, projecting posteriorly and not enclosing the groove. The posterior intercondylar groove extends for less than one-quarter of the femoral length, a condition comparable to that of *Koreanosaurus* (Huh et al. 2011), *Oryctodromeus* (Krumenacker et al. 2023), *Jeholosaurus* (Han et al. 2012), *Parksosaurus* (Sues et al. 2023), and *Thescelosaurus* (Gilmore 1915; Morris 1976; Brown et al. 2011), but differing from *Orodromeus* (Scheetz 1999) and *Haya* (Makovicky et al. 2011; Barta and Norell 2021). In contrast, an anterior (extensor) intercondylar groove is absent, distinguishing this specimen from *Zephyrosaurus* (Sues 1980) and *Thescelosaurus neglectus* (Gilmore 1915). The distal condyles are oriented perpendicularly relative to the shaft axis and are subequal in anteroposterior expansion. However, the medial condyle is slightly broader than the lateral one, resembling the condition in *Parksosaurus* (Sues et al. 2023), while the other early-diverging neornithischians exhibit subequal condyles. The transverse widths of the medial condyle and the crista tibiofibularis are subequal, differing from the condition in *Koreanosaurus* (Huh et al. 2011), *Orodromeus* (Scheetz 1999), *Zephyrosaurus* (Sues 1980), *Haya* (Makovicky et al. 2011; Barta and Norell 2021), *Parksosaurus* (Sues et al. 2023), and *Thescelosaurus neglectus* (Gilmore 1915). The surface between the lateral condyle and the crista tibiofibularis is smooth to shallowly grooved, a morphology shared with *Koreanosaurus* (Huh et al. 2011), *Oryctodromeus* (Krumenacker et al. 2023), *Haya* (Makovicky et al. 2011; Barta and Norell 2021), *Jeholosaurus* (Han et al. 2012), *Thescelosaurus neglectus* (Gilmore 1915), and *Th. assiniboiensis* (Brown et al. 2011).

The left tibia is preserved from the midshaft to the proximal end (Fig. 12A). In cross-section, the tibial shaft is rounded, resembling the condition in *Koreanosaurus* (Huh et al. 2011), *Jeholosaurus* (Han et al. 2012), and *Parksosaurus* (Sues et al. 2023), but differing from the triangular morphology of *Fona* (Avrahami et al. 2024), *Oryctodromeus* (Krumenacker et al. 2023), *Thescelosaurus* (Gilmore 1915; Morris 1976; Brown et al. 2011), *Orodromeus* (Scheetz 1999), and *Haya* (Makovicky et al. 2011; Barta and Norell 2021).

The proximal end of the tibia has well-developed lateral and medial condyles that are distinctly separated by a deep notch (Fig. 12A). The lateral condyle is offset anteriorly relative to the medial condyle and is larger or subequal in width to the posterior condyle, as in *Albertadromeus* (Brown et al. 2013), *Koreanosaurus* (Huh et al. 2011), *Jeholosaurus* (Han et al. 2012), and *Parksosaurus* (Sues et al. 2023), but unlike *Orodromeus* (Scheetz 1999), *Oryctodromeus* (Krumenacker et al. 2023), and *Changchunsaurus* (Butler et al. 2011). In anteroposterior view, the lateral condyle defines an abrupt overhanging buttress with a subhorizontal ventral margin, a feature shared with *Fona* (Avrahami et al. 2024), *Oryctodromeus* (Krumenacker et al. 2023), and *Orodromeus* (Scheetz 1999), but absent in *Changchunsaurus* (Butler et al. 2011) and *Parksosaurus* (Sues et al. 2023). No accessory condyle is developed on the lateral side, similar to the condition in *Parksosaurus* (Sues et al. 2023) and

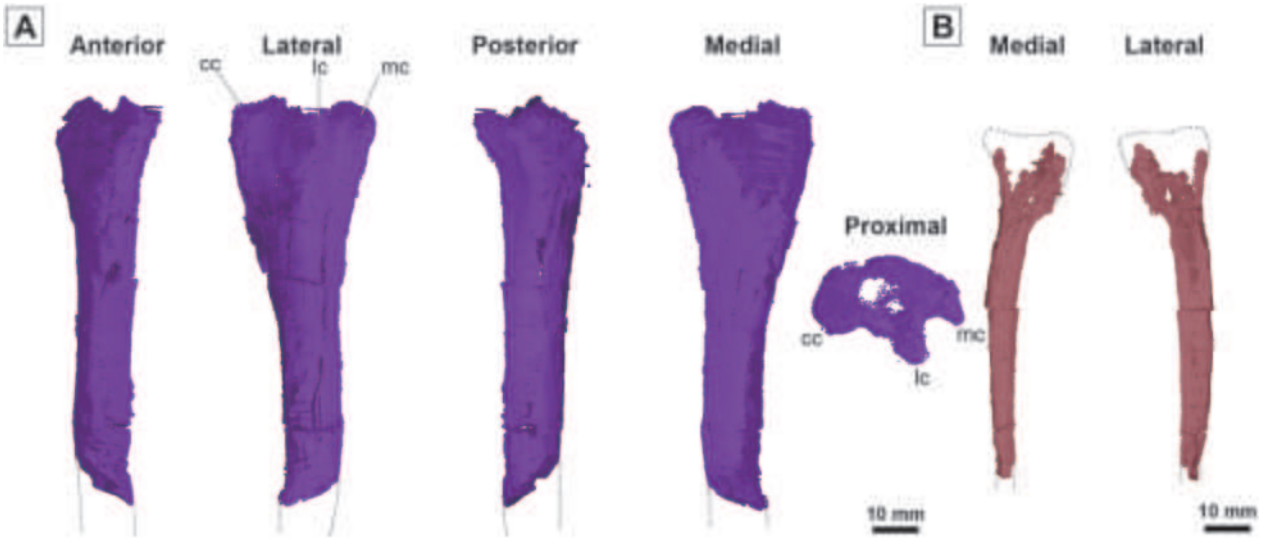

Figure 12. Left **A.** Tibia and **B.** Fibula of KDRC-SA-V001. Abbreviations: cc: cnemial condyle; lc: lateral condyle; mc: medial condyle.

Thescelosaurus assiniboiensis (Brown et al. 2011). The cnemial crest is prominent, curving anterolaterally and appearing rounded in lateral view, a morphology typical of early-diverging neornithischians. The medial surface of the proximal tibia forms a continuous arc along the anteroposterior axis in proximal view.

The proximal left fibula is preserved from the midshaft in articulation with the tibia (Fig. 12B). However, much of the detailed anatomical morphology of the proximal end of the fibula is difficult to discern. It is expanded both medially and laterally, and its anterior edge arcs anteromedially, a condition typical of early-diverging neornithischians. In cross-section, the fibular shaft is D-shaped, which contrasts with the more rounded condition described in *Thescelosaurus neglectus* (Gilmore 1915) and *Th. garbanii* (Morris 1976).

Metatarsals I-III of the left foot are partially preserved in KDRC-SA-V001 (Fig. 13). Considering the typical early-diverging neornithischian digit formula (2-3-4-5-0) (Avrahami et al. 2024) and that the length of phalanx II-1 exceeds that of IV-1, the articulated metatarsals and digits are identified as belonging to the left pes. They are closely appressed, as in other early-diverging neornithischians. However, metatarsal I is highly damaged, providing little morphological information. Metatarsal II is represented only by its distal portion. Its ventral surface is gently arched dorsally. A shallow collateral ligament pit is visible, but the ginglymoid distal articular surface of this metatarsal is damaged. The distal half of metatarsal III is preserved and broadens slightly toward the distal end. In cross-section, it is elliptical, with the right lateral surface curving more medially than the left. Its ginglymoid articular surface is more strongly expressed ventrally than dorsally; a shallow collateral ligament pit is present.

All phalanges of pedal digits II and III are well preserved and articulated, whereas digit I preserves only one phalanx, and those of digit IV are not preserved (Fig. 13). Digits II and III consist of three and four phalanges, respectively, consistent with the typical early-diverging neornithischian phalangeal formula of 2-3-4-5-0 (Avrahami et al. 2024). All preserved phalanges are elongated and cylindrical, with expanded proximal and distal ends and a relatively thin midshaft. The first phalanges (II-1 and III-1) are longest, with subsequent phalanges decreasing in length. The distal articular surfaces bear well-developed condyles, more distinct ventrally, and possess deep collateral ligament pits laterally and medially. Notably, the dorsodistal surface of phalanx II-1 bears a distinct fossa (Fig. 13; ep). This fossa is also present in *Changmiania* (Yang et al. 2020), *Oryctodromeus* (Krumenacker et al. 2023), and *Changchunsaurus* (Butler et al. 2011). The proximal articular facets change in morphology from a single surface on the first phalanges to bifaceted surfaces separated by a medial ridge on the second and third phalanges.

The ungual of digit III is preserved in partial articulation, whereas an isolated ungual likely belongs to digit II based on size (Fig. 13). Both unguals are claw-like, being longer than wide, with pointed distal ends and dorsally arched dorsal and ventral margins. Longitudinal grooves are present on the medial and lateral surfaces. The ungual of digit II is narrower and more slender than that of digit III, whereas the ungual of digit III exhibits a more strongly curved ventral surface. Flexor tubercles are absent or expressed only as a low mound adjacent to the articular surface.

Gastroliths. Forty to fifty small and well-sorted subangular pebbles and similarly sized discoid stones occur in a cluster between the vertebrae and femur of specimen KDRC-SA-V001 (Fig. 14A, B). These pebbles exhibit smooth surfaces and consist of diverse lithologies, including quartzite and volcanic rocks. Some of the dark volcanic pebbles are oblong in shape, whereas those of quartzite tend to exhibit a more spherical morphology. The size of individual pebbles ranges from 2 to 10 mm

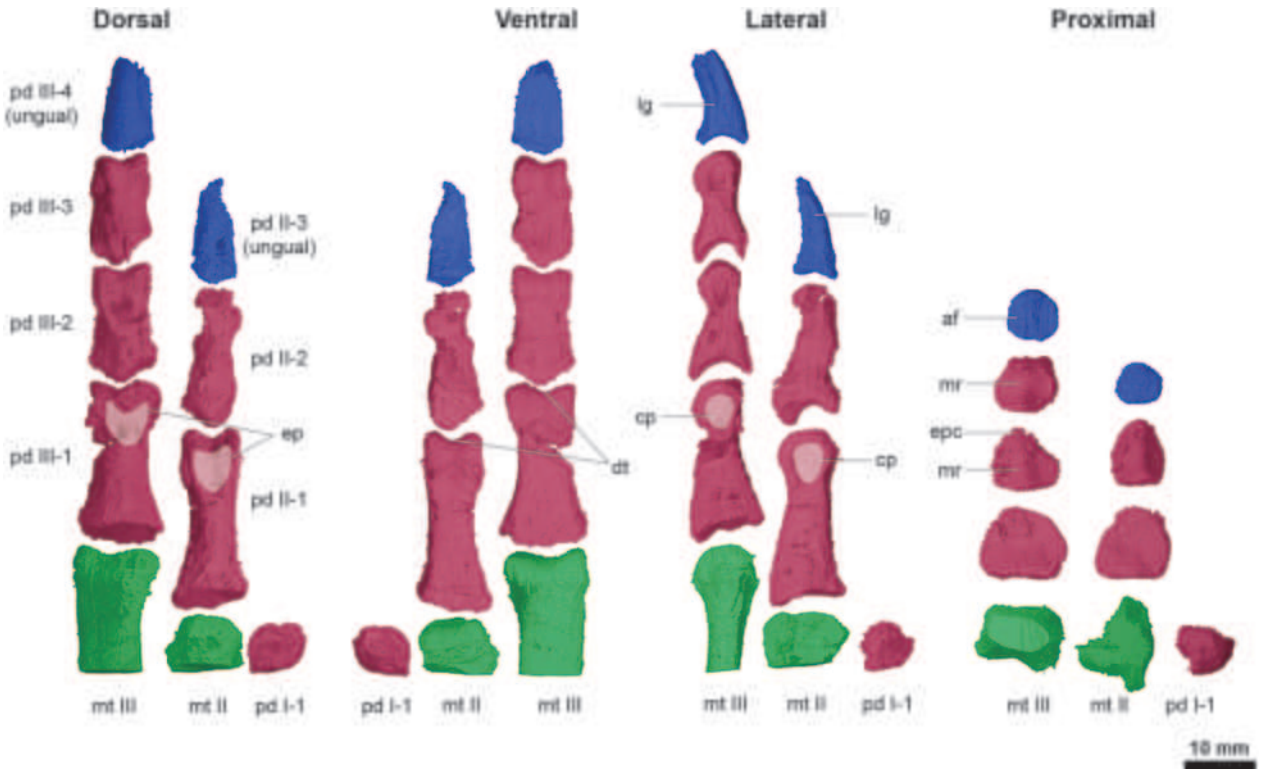

Figure 13. Left pes of KDRC-SA-V001. Abbreviations: af: articular facet; cp: collateral pit; dt: distal trochlea; ep: extensor pit; epc: extensor process; lg: longitudinal groove; mr: medial ridge; mt: metatarsal; pd: pedal digit.

in diameter, and the cluster forms an approximately ellipsoidal mass with principal axes of 12 mm, 12 mm, and 31 mm. The total volume of the gastroliths is estimated at 9.3 mL. Considering that several pebbles are exposed at the surface, the actual volume was likely greater. Based on the average density of silicate rocks (3.3 g/cm^3), the total mass of the gastroliths is estimated at a minimum of 30.7 g. Comparable occurrences of clustered gastroliths have been documented in closely related taxa such as *Haya* (Makovicky et al. 2011; Barta and Norell 2021) and *Changmiania* (Yang et al. 2020), but have not been reported in any North American thescelosaurid taxa.

Histological data. In *Doolysaurus*, the transverse femoral thin section reveals a thin cortical wall measuring 1.2–1.6 mm in thickness (Fig. 15). Although the outermost cortex in some areas is damaged, the preserved regions allow limited assessment of the primary histological structure. The cortical tissue consists of parallel-fibered bone containing primarily longitudinal vascular canals. The density of vascular canals shows no significant difference between the inner and outer cortex. A faint, lighter-colored transverse line occurs near the mid-cortex, but its alignment with a crack in the section and the differing texture surrounding it make its interpretation unclear; it may represent a line of arrested growth (LAG) (Fig. 15B, C). There is no indication of significantly reduced vascularization toward the external surface, suggesting that the individual was still undergoing relatively rapid growth at the time of death.

Phylogenetic results. Both parsimony and tip-dated Bayesian analyses of the Fonseca et al. (2024) dataset recover Thescelosauridae as a monophyletic group and *Doolysaurus huhmini* within this clade (Suppl. material 1: figs S1–S4). In the Bayesian analysis, *Doolysaurus* is recovered in Thescelosaurinae as the sister taxon of a clade including *Parksosaurus*, *Fona*, and *Thescelosaurus* (Fig. 16). Parsimony analysis yielded 381 equally most parsimonious trees (tree length of 7081). In the strict consensus of these trees, relationships within Thescelosauridae are unresolved; *Doolysaurus* forms part of a large polytomy (Suppl. material 1: fig. S1). In the 50% majority-rule consensus, *Doolysaurus* also lies within a monophyletic Thescelosaurinae that contains *Parksosaurus*, *Fona*, and *Thescelosaurus*. This clade also includes additional small-bodied species from Asia (Suppl. material 1: fig. S2); *Changmiania*, rather than being recovered as the sister taxon to all other Thescelosauridae (Fig. 16), is placed within Thescelosaurinae as the most basally divergent taxon within that clade (Suppl. material 1: fig. S2). A clade comprising other Asian taxa (*Jeholosaurus*, *Changchunsaurus*, *Haya*, and *Yueosaurus*), like that reported by Fonseca et al. (2024), is recovered as the sister taxon to a *Fona*, *Parksosaurus*, and *Thescelosaurus* clade within Thescelosaurinae (Suppl. material 1: fig. S2). In both the Bayesian analysis and the 50% majority-rule consensus tree from the parsimony analyses, *Koreanosaurus* is recovered within Orodrominae as the only Asian taxon in this clade. This position has been recovered in previous analyses (Boyd 2015; Fonseca et al. 2024; Avrahami et al. 2024).

To test the sensitivity of the recovered phylogenetic position of *Doolysaurus huhmini*, we additionally employed the recently published matrix of Avrahami

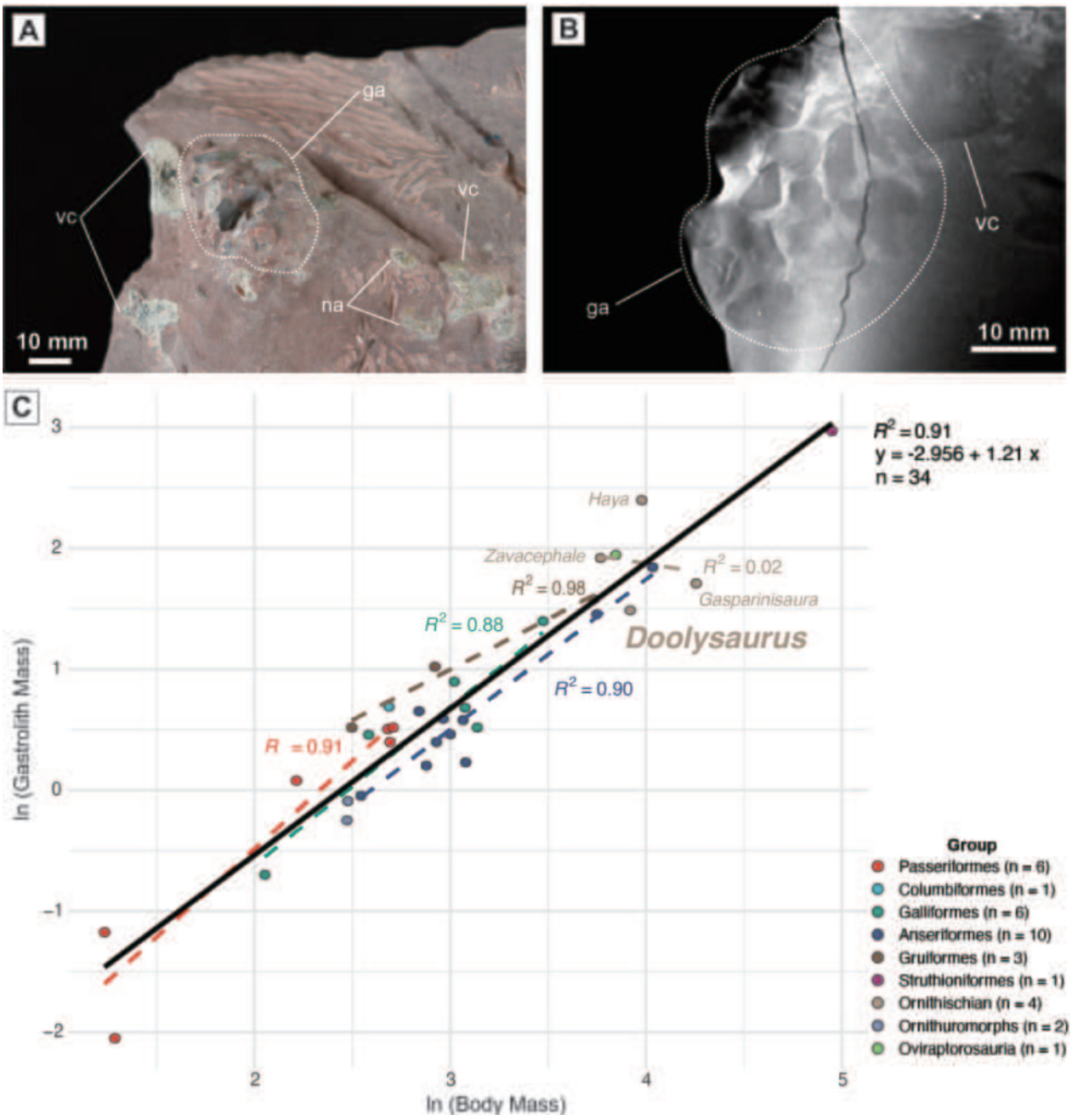

Figure 14. Gastroliths of KDRC-SA-V001. **A.** Exposed gastrolith mass of KDRC-SA-V001; **B.** CT-scanned image of the gastroliths; **C.** Relationship between body mass and gastrolith mass in dinosaurs, including extant birds. Dotted lines indicate the regression line for each group with more than three samples, and the black line represents the regression line for the total dataset. Gastrolith and body mass data follow the dataset compiled by Wings and Sander (2007), Cerda (2008), Makovicky et al. (2011), Liu et al. (2023), and Chinzorig et al. (2025). The gastrolith mass of *Doolysaurus* is a minimum value (see text), and the estimated body mass is based on femoral circumference using the equation of Campione et al. (2014). Abbreviations: ga: gastrolith; na: neural arch; vc: vertebral centrum.

et al. (2024). In tip-dated Bayesian analyses, the topology is poorly resolved, showing multiple polytomies within Neornithischia (posterior probability > 0.5). Under a relaxed threshold (posterior probability > 0.1), Thescelosauridae is resolved as a monophyletic group, and *Doolysaurus* falls within this clade. The parsimony analysis yielded 12 equally most parsimonious trees with a best score (TBR) of 1834. Thescelosauridae is not recovered as monophyletic in the strict consensus tree but forms a clade in the 50% majority-rule consensus. In this tree, *Jeholosaurus*, *Parksosaurus*, *Yueosaurus*, and *Changchunsaurus* are placed outside Thescelosauridae. *Doolysaurus* forms a node with *Diluvicursor* as a basal member of Orodrominae within Thescelosauridae, while *Koreanosaurus* forms a node with *Micropachycephalosaurus* within Thescelosaurinae.

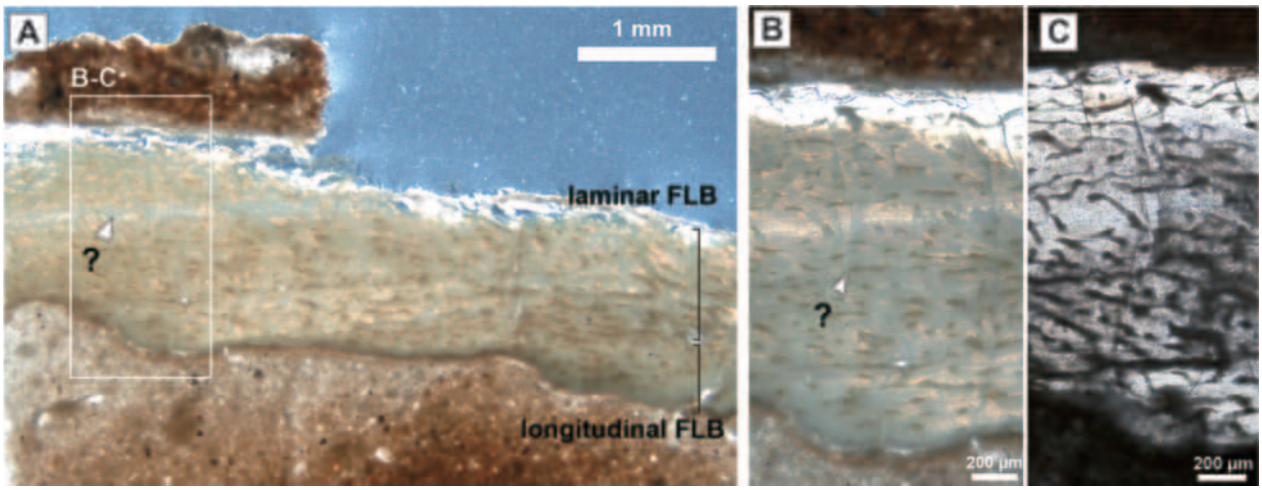

Figure 15. Histological thin-section images of the femoral cortex of KDRC-SA-V001. **A.** Cross-section of the anterolateral region of the femur; **B, C.** Magnified view of the cortical bone under plane-polarized light (**B**) and cross-polarized light with mineral oil coating (**C**). Abbreviations: FLB: fibrolamellar bone; LAG: line of arrested growth.

Notably, in both the Fonseca et al. (2024) and Avrahami et al. (2024) datasets, in all analyses in which Thescelosauridae is resolved, the Asian taxa, including *Doolysaurus*, consistently occupy basal positions within the group or form basal branches within either Orodrominae or Thescelosaurinae.

Doolysaurus shares two synapomorphies of Thescelosaurinae proposed by Fonseca et al. (2024): a fossa on the base of the pterygoid wing of the quadrate [ch. 195:1] and an overhanging tibia lateral condyle [ch. 842:1]. Although the precise composition of this clade has varied across studies and analyses, it generally includes the North American taxa, including *Thescelosaurus*, *Parksosaurus*, and *Fona*, and more basal Asian taxa, including *Haya*, *Changchunsaurus*, and *Jeholosaurus* (Boyd 2015; Fonseca et al. 2024). In contrast, *Koreanosaurus* has consistently been recovered as a member of Orodrominae (Boyd 2015; Madzia et al. 2018; Barta and Norell 2021; Krumenacker et al. 2023; Sues et al. 2023; Avrahami et al. 2024; Fonseca et al. 2024), and in our revised analysis, based on the modification of new characters, was again nested within Orodrominae.

Discussion

Paleobiogeography of the thescelosaurids in the Cretaceous of Korea

While the origin of Neornithischia has been hypothesized to be in Africa, their subsequent diversification has been estimated to have taken place within Asia (Boyd 2015). However, whether the divergence of Thescelosaurinae and Orodrominae occurred in Asia or in North America remains unresolved; Boyd (2015) noted that likelihood-based analyses suggested that the basal-most divergence of Thescelosauridae most likely occurred in North America during the Aptian, but the results of the parsimony-based analysis (PB) could not resolve whether the split more likely took place in North America or Asia. In our phylogenetic analyses, both parsimony and tip-dated Bayesian analyses show that *Doolysaurus* has closer affinities to North American taxa such as *Parksosaurus*, *Fona*, and *Thescelosaurus* than to other basal East Asian groups, such as *Haya*, *Changchunsaurus*, and *Jeholosaurus* (Fig. 16, Suppl. material 1: fig. S2). Although the phylogenetic positions and specific clade compositions vary among analyses, results from both the Fonseca et al. (2024) and Avrahami et al. (2024) datasets consistently show that whenever Thescelosauridae is recovered as a monophyletic group, the Asian taxa occupy more basal positions relative to the North American taxa (Fig. 16, Suppl. material 1: figs S2, S8). This suggests that the initial divergence of Thescelosaurinae and Orodrominae may have occurred in Asia, followed by dispersal into North America. Notably, *Koreanosaurus* represents the only known occurrence of Orodrominae outside North America (Boyd 2015). Boyd (2015) suggested that *Koreanosaurus* could have dispersed from North America back into East Asia via Beringia during or before the Cenomanian.

Doolysaurus was recovered from the Albian–early Cenomanian (~113–97 Ma) Ilseongsan Formation of Shinan, whereas *Koreanosaurus* was discovered in the younger Seonso Conglomerate (81 Ma) of Boseong (Kim et al. 2008). In the North American record, thescelosaurines and orodromines rarely occur in the same deposits (Avrahami et al. 2024). There, thescelosaurines, such as *Parksosaurus* and *Thescelosaurus*, were traditionally thought to appear only near the end of the Cretaceous. In contrast, orodromines, such as *Orodromeus*, *Albertadromeus*, *Zephyrosaurus*, and *Oryctodromeus*, were known from the Albian to Campanian. This discrepancy raised questions about the long ghost lineage of thescelosaurines (Boyd 2015). However, recent

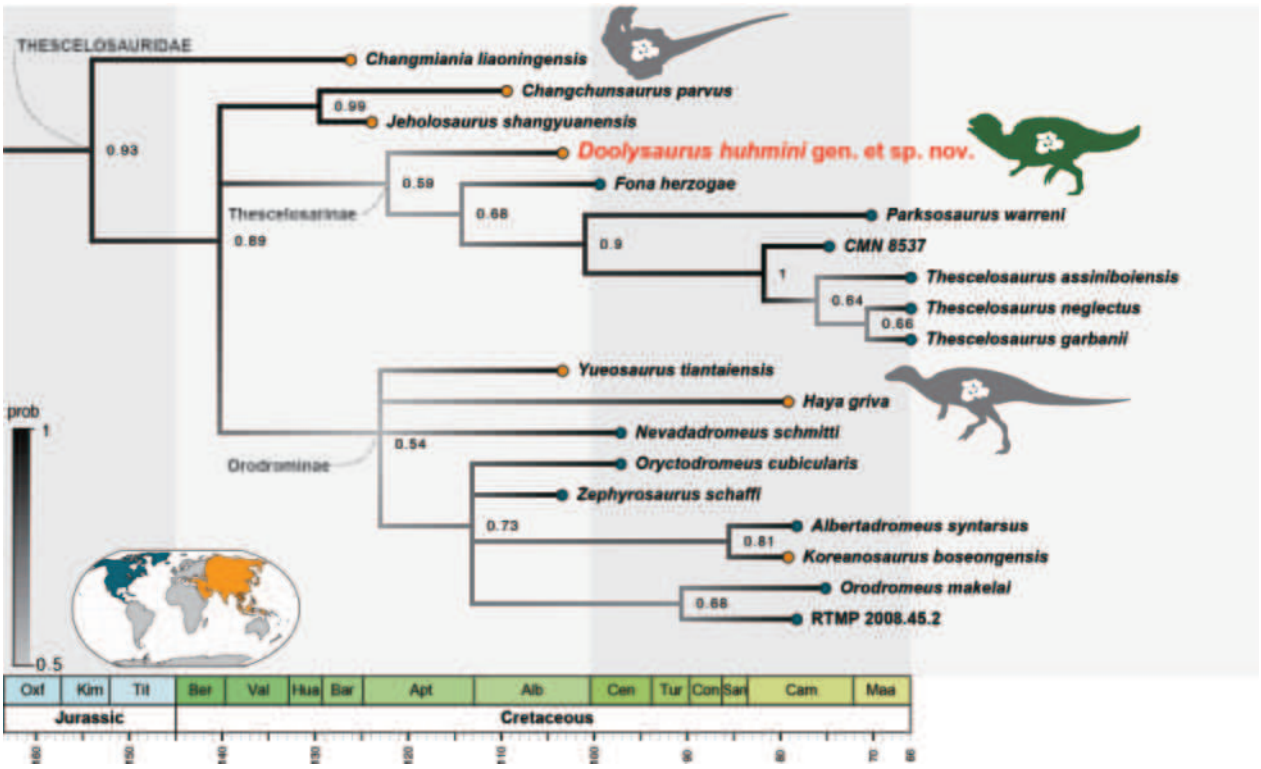

Figure 16. Phylogenetic tree of Thescelosauridae from the tip-dated Bayesian analysis of the character matrix of Fonseca et al. (2024), showing the position of *Doolysaurus* and scaled to geological time. Small numbers at nodes are posterior probabilities. The color of each tip node corresponds to the continent where the fossil was discovered. Taxa with documented gastroliths (*Changmiania*, *Haya*, and *Doolysaurus*) are highlighted with silhouettes. Tip ages were constrained following the mean of the minimum and maximum ages from the Paleobiology Database (PBDB; http://paleobiodb.org) and Avrahami et al. (2024), with the tip age of *Doolysaurus huhmini* fixed at 103.45 Ma, corresponding to the midpoint between the Albian and Cenomanian. *Doolysaurus huhmini* is recovered within Thescelosaurinae, forming a clade with *Fona*, *Parksosaurus*, and *Thescelosaurus*.

discoveries of *Fona* from the Cedar Mountain Formation (Cenomanian) and reinterpretation of *Oryctodromeus* as a potential thescelosaurine demonstrate that both thescelosaurines and orodromines coexisted in North America during the Late Cretaceous (Avrahami et al. 2024). Despite this temporal overlap, they have not yet been recovered from the same localities, suggesting possible differences in their preferred paleoenvironmental settings (Avrahami et al. 2024). However, it remains unclear whether the spatiotemporal separation of the two Korean thescelosaurids may further inform the ecological differentiation proposed for the clade or reflect secondary dispersal of orodromines back into Asia; additional fossil evidence is required.

Ontogenetic stage of the *Doolysaurus* holotype

The holotype of *Doolysaurus* exhibits several features that indicate it may represent an early ontogenetic stage. First, all vertebral elements are preserved with the centra separated from the neural arches (Fig. 9). The degree of neurocentral suture closure is widely recognized as an indicator of skeletal maturity in dinosaurs (Brill and Carpenter 2001; Irmis 2007; Hone et al. 2016). Although information on the neurocentral suture fusion sequence in ornithischians remains largely unknown (Irmis 2007; Griffin et al. 2021), the fact that many centra and neural arches remain unfused and separated indicates that this individual was not a fully grown adult. In addition, although the hindlimb elements (femur, tibia, fibula, metatarsals, and phalanges) are well articulated, the cranial elements are disarticulated and scattered. This likely reflects the fact that ossification and fusion of the cranial elements were not yet completed. Similar patterns of cranial disarticulation in juvenile individuals relative to the postcranial skeleton have been reported in other early-diverging neornithischians (Hübner and Rauhut 2010; Snyder et al. 2020). The strongly bowed morphology of the femur (Fig. 11) may also support a juvenile condition (Weishampel et al. 2003). Although bipedal early-diverging neornithischians generally exhibit a more anteriorly bowed femur than quadrupedal large-bodied ornithopods (Pintore et al. 2025), ontogenetic variation in the degree of anterior curvature from more bowed to less bowed has been documented within several taxa, including *Tenontosaurus*, *Zalmoxes*, and *Camptosaurus* (Weishampel et al. 2003). The femur of *Doolysaurus* appears even more strongly bowed than that of most adult early-diverging neornithischians. However, it is similar to the morphology in *Haya*, a taxon in which similar bowing of the femoral shaft was observed in both

adults and juveniles (Barta and Norell 2021). It is worth noting, however, that sensitivity analyses investigating the impact of changing the scoring of this character to unknown did not change the placement of *Doolysaurus* in the phylogenetic analyses.

Comparison of the body size of the individual represented by the *Doolysaurus* holotype specimen, combined with histological data from the femur, suggests that this specimen most likely represents a juvenile individual. Numerous histological studies on small-bodied neornithischians facilitate more reliable comparative assessments of ontogenetic stages for individuals of distinct sizes (Scheetz 1999; Horner et al. 2009; Hübner 2010, 2012; Kim et al. 2017; Krumenacker 2017; Cruzado-Caballero et al. 2019; Han et al. 2020; Barta and Norell 2021; Nogueira et al. 2024; Avrahami 2025). The relative size of *Doolysaurus* was estimated using the width and circumference of the femoral midshaft. The anteroposterior and mediolateral diameters of the femoral midshaft are 15.79 mm and 14.51 mm, respectively, and the circumference is 14.90 mm. Based on regression analyses derived from Australian ornithopod femora (Kitchener et al. 2019), the estimated total femoral length of *Doolysaurus* is approximately 12–13 cm. Comparable femoral lengths are reported in specimens of *Fona* (NCSM 33545, 12.25 cm), *Haya* (IGM 100/2015, 12.9 cm), and *Dryosaurus* (MWC 1477-F5-1, estimated 14 cm). Among these, those from *Fona* (Avrahami 2025) and *Dryosaurus* (Horner et al., 2010) also show no LAGs, while *Haya* exhibits two such lines (Barta and Norell 2021). The smallest *Dysalotosaurus* (GPIT/RE/4156r, 8.5 cm) is even smaller, but no histological data were available from this specimen (Hübner 2010; Hübner et al. 2021).

Gastroliths in early-diverging neornithischians

Although gastrolith occurrences are relatively rare in Ornithischia compared to those in avian and non-avian theropods and sauropods, recent studies have reported their presence in distinct taxa, such as Ceratopsia, Ankylosauria, Stegosauria, and Ornithopoda (Wings 2004; Takasaki 2020; Chinzorig et al. 2025). Clear evidence of gastroliths in early-diverging ornithischians has been documented in *Gasparinisaura* (Cerda 2008), *Haya* (Makovicky et al. 2011; Barta and Norell 2021), *Changmiania* (Yang et al. 2020), as well as now *Doolysaurus*. The occurrence of gastroliths in *Doolysaurus* provides further evidence that the use of gastroliths among early-diverging, small-bodied neornithischians was a more common feature.

In *Doolysaurus*, the total mass of gastroliths is approximately 30.7 g, while its total body mass, estimated from femoral circumference following Campione et al. (2014), is about 8.3 kg. This corresponds to roughly 0.37% of the total body mass. We find that for ornithischian dinosaurs in which gastrolith mass has been estimated, including *Doolysaurus*, *Haya*, *Gasparinisaura*, and *Zavacephale*, the relationship between body mass and gastrolith mass appears to show a strong linear correlation ($r^2 = 0.90$) (Fig. 14C), which is also consistent with predictions from a regression derived from scaling in extant frugivorous and granivorous avian taxa (Wings and Sander 2007).

The gastroliths of *Doolysaurus* are subrounded, resembling those in *Haya* and *Psittacosaurus* (Takasaki 2020) (Fig. 14A, B). Such gastrolith morphology indicates that *Doolysaurus* likely had a less powerful muscular gastric mill than that of modern granivorous birds (Best and Gionfriddo 1991). Similarly, gastroliths reported in *Changmiania* show a subangular morphology with a smooth patina (Yang et al. 2020). In addition, the occurrence of numerous discoid pebbles with spherical-shaped ones suggests possible dietary flexibility and a feeding ecology more comparable to that of extant omnivorous birds (Best and Gionfriddo 1991). The morphology of gastroliths observed in *Doolysaurus* and other early-diverging neornithischians may indicate a generalized or omnivorous dietary strategy for this group. However, extant birds exhibit considerable variation in stomach anatomy and gastrolith usage across clades (Takasaki and Kobayashi 2024), suggesting that caution is required when utilizing these data to infer the diets of non-avian dinosaurs. Additional fossil and extant specimens of diverse reptilian groups and further quantitative analyses are needed to understand the relationship between gastrolith mass, morphology, and diet.

Trace fossil record discrepancy in early-diverging neornithischian

Although several skeletal specimens of early-diverging neornithischians, including *Doolysaurus*, have been reported from the Cretaceous of Korea, no tracks attributed to this group have been documented (Kim and Huh 2018). The absence of footprints from this clade may result from a mismatch between habitat and sampled depositional environments. The sedimentary contexts of *Doolysaurus* and *Koreanosaurus* are interpreted as floodplain deposits characterized by the development of paleosols (Paik et al. 2004), which means the substrate remained subaerially exposed for an extended duration under unsaturated conditions. Such a depositional environment is not conducive to preserving footprint fossils, as it does not meet the conditions required for their preservation, which typically involve brief subaerial exposure followed by rapid burial. Furthermore, many early-diverging neornithischians are inferred to have exhibited fossorial or semi-fossorial behaviors (e.g., Varricchio et al. 2007; Huh et al. 2011; Fearon and Varricchio 2015; Button and Zanno 2023; Avrahami et al. 2024). Because most digging behavior in terrestrial animals occurs under subaerial conditions rather than in water-saturated substrates, such settings differ significantly from the typical footprint-preserving environments, such as lake margins or shorelines. Thus, an ecological and sedimentological mismatch could help

explain the absence of their footprints in the Korean Cretaceous track record.

Alternatively, it is also possible that footprints attributable to early-diverging neornithischians may have been misidentified as those of theropods. Although the pes of early-diverging neornithischians typically comprises four digits, the functional significance of digit I in locomotion remains uncertain. In particular, several taxa exhibit a reduced metatarsal I, and phalanx I-1 is shorter than metatarsal II (Fonseca et al. 2024: character 911). This condition is especially evident among Asian taxa such as *Jeholosaurus*, *Changmiania*, and *Changchunsaurus*, which possess a reduced metatarsal I compared to their North American counterparts, including *Thescelosaurus*, *Parksosaurus*, *Orodromeus*, and *Fona*. In such cases, digit I likely did not make contact with the substrate during locomotion, resulting in a tridactyl, digitigrade footprint morphology that closely resembles that of theropods.

Several ichnotaxa, such as *Ateripus*, *Deltatorrichnus*, and *Hypsiloichnus* (Gierliński and Karol 2008), as well as tracks from Las Cerradicas, Spain (Castanera et al. 2013), have been attributed to early-diverging neornithischians. These assignments are based on features such as the presence of manus impressions or digit IV in the pes track (e.g., *Hypsiloichnus*). However, Castanera et al. (2013) highlighted the inherent difficulty in distinguishing footprints of early-diverging neornithischians from those of theropods due to their morphological similarity, such as long and slender three functional digits. In addition, given that many small-bodied neornithischians were likely bipedal (Maidment and Barrett 2012; Maidment et al. 2012; Barrett and Maidment 2017; Pintore et al. 2025), it is plausible that early-diverging neornithischians may instead have produced some bipedal, sharp, tridactyl digitigrade footprints previously assigned to theropods.

Dinosaur body fossil record and preservation bias in Korea

The rarity of well-preserved dinosaur skeletons in Korea may be explained by a combination of geological, taphonomic, and geographical factors. Most Mesozoic body fossil-bearing strata in Korea are exposed in coastal and island regions, such as Boseong, Hadong, and Shinan, where strong tidal activity and limited terrestrial access hinder systematic excavations. Moreover, widespread magmatism during the Late Cretaceous to early Paleogene (Sagong et al. 2005; Chough and Sohn 2010; Park 2012) caused thermal metamorphism of many sedimentary rocks into hornfels and tectonic deformation of sedimentary sequences, severely compromising fossil preservation and rendering mechanical preparation difficult (Kim and Huh 2018).

Considering the diversity of the extensive Korean dinosaur footprint record, the actual diversity of the Cretaceous dinosaur fauna was far greater than is currently represented by the body fossil record. The presence of footprints attributed to diverse-sized Ankylopollexia (e.g., Paik et al. 2006; Hwang et al. 2008; Lockley et al. 2012; Yoon et al. 2021), Ankylosauria (Yoon et al. 2026), and a wide size range of non-avian theropods (e.g., Huh et al. 2003; Kim et al. 2018; Kim et al. 2019) suggests the existence of multiple taxa, but their body fossils have not yet been recorded from skeletal remains. In particular, bird traces from the latest Early to Late Cretaceous exhibit remarkable diversity and abundance (Kim and Huh 2018), yet skeletal remains have not been discovered in similarly aged rocks on the Korean Peninsula.

The Aphaedo site yields not only a large, well-preserved theropod egg nest but also a small, articulated early-diverging neornithischian skeleton, preserved in delicate detail and likely reflecting distinct depositional and diagenetic conditions. Other Korean dinosaur body fossil-bearing localities have so far yielded generally more fragmentarily preserved remains (Fig. 17). This site holds unique promise for key insights into not only the mid-Cretaceous evolution and radiation of early-diverging neornithischians, bridging the gap between the Early Cretaceous (e.g., Yixian Formation, China) and the Late Cretaceous (e.g., Javkhlant Formation, Mongolia), but also other clades. Given this exceptional preservation potential, the Aphaedo site and other sites with comparable depositional and taphonomic settings may yield additional, well-preserved skeletons in future discoveries, offering new insights into the diversity and paleoecology of the Cretaceous Korean dinosaur fauna.

Conclusion

Doolysaurus huhmini from the Ilseongsan Formation (Albian–Cenomanian) on Aphaedo Island, Shinan, represents the second early-diverging neornithischian taxon described from Korea and the first diagnostic cranial materials of a dinosaur from the Korean Peninsula. The anatomical features and phylogenetic analyses of *Doolysaurus* indicate that it represents a juvenile thescelosaurine. The species adds to growing evidence that early diversification in Thescelosauridae, including the split between Thescelosaurinae and Orodrominae, may have occurred in Asia, with subsequent early dispersal to North America. Gastroliths associated with *Doolysaurus* share morphological characters with those of *Haya* and *Psittacosaurus* and resemble those of modern omnivorous birds, supporting the inference of a generalized or omnivorous dietary strategy in early-diverging neornithischians. Furthermore, the absence of definitive footprint fossil records attributed to early-diverging neornithischians in Korea may reflect habitat preference and preservational bias or misidentification with theropod tracks due to similar pedal morphology. The co-occurrence of an exceptionally large oviraptorosaurian egg nest and delicate, small-bodied neornithischian remains at the Aphaedo site underscores its importance as a newly recognized dinosaur body fossil locality.

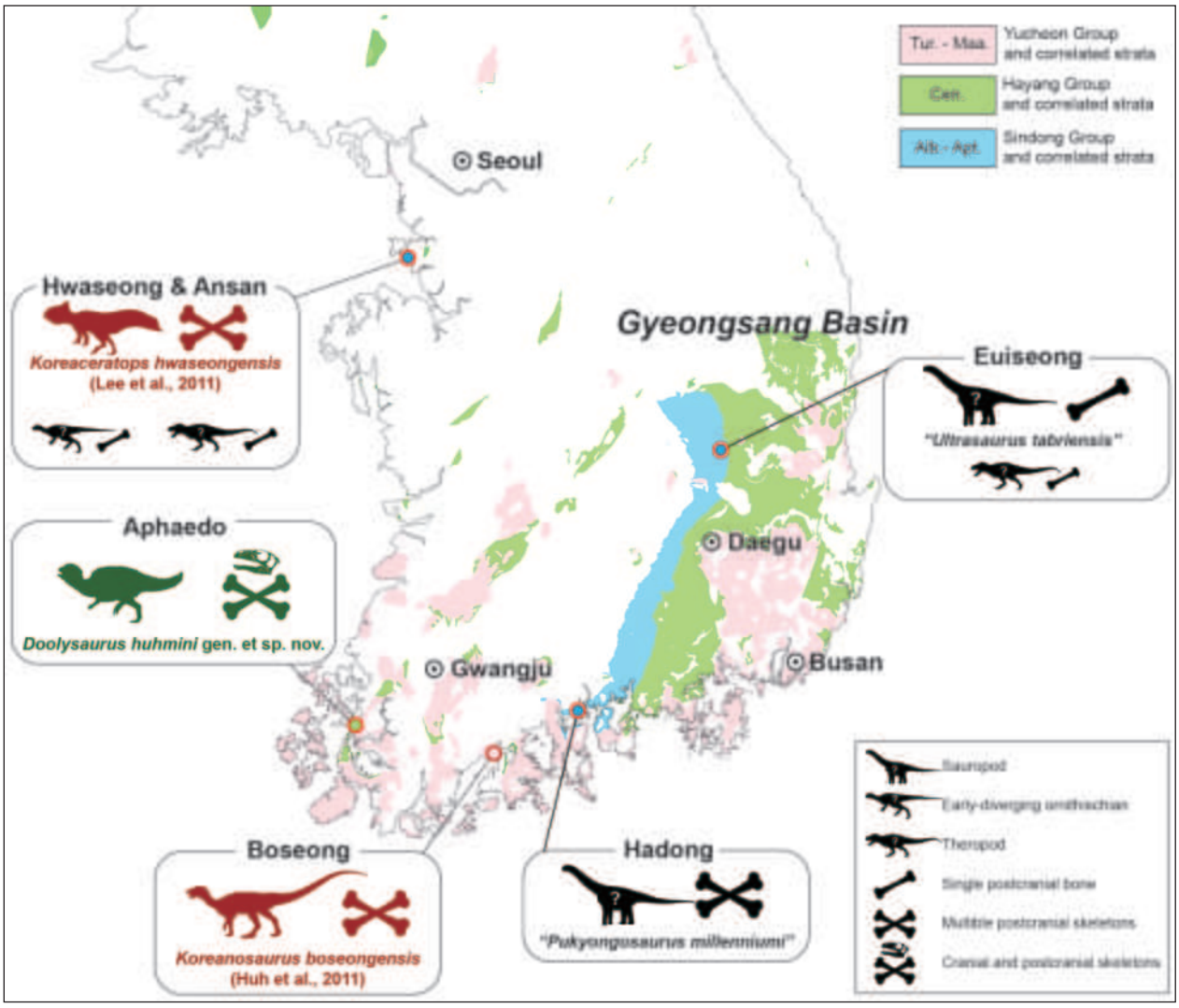

Figure 17. Distribution of dinosaur skeletal fossil records in Korea, including *Doolysaurus huhmini* from Aphaedo. Colored silhouettes and labels indicate valid taxa, whereas question-marked silhouettes in black represent uncertain or invalid taxa. Silhouettes of sauropods, early-diverging neornithischians, and theropods are from http://phylopic.org.

Acknowledgments

We appreciate the helpful comments from reviewers Daniel E. Barta and Christian Foth and editor Florian Witzmann that improved this manuscript. We are grateful to Jessica A. Maisano, David Edey, and Matthew Colbert (University of Texas High-Resolution X-ray Computed Tomography Facility; UTCT) for their assistance with micro-CT scanning. We thank Carmen Urban for technical assistance with CT segmentation methods. We also thank Jae-Il Park and Hye-Yeon Jung (Korea Basic Science Institute) for their help with micro-CT scanning. We thank Janet Cañamar (University of Texas at Austin) for the reconstruction and Lucas Legendre (University of Texas at Austin) for insightful discussions and advice on histological interpretations and manuscript preparation. We acknowledge Seong Young Ju (Shinan County Office), Bo Seong Kim (Mokpo Natural History Museum), and Beom Geun Cha (FITI Testing & Research Institute) for their contributions during fieldwork and excavation. We also thank Jieun Park (Chonnam National University) for assistance with mechanical preparation. We are also indebted to Min Su Kang (Chonnam National University) for taking thin-section images. The material in this study was excavated during "*A Research on the Dinosaur Egg Fossil Site in Aphae Island, Shinan,*" commissioned by Shinan-gun County.

References

Avrahami HM (2025) The Anatomy, Phylogeny, Ontogeny, and Histology of the Semi-Fossorial thescelosaurid dinosaur—*Fona herzogae*—from The Cenomanian-age Mussentuchit Member of the Cedar Mountain Formation, Utah. North Carolina State University, 367 pp.

Avrahami HM, Makovicky PJ, Tucker RT, Zanno LE (2024) A new semi-fossorial thescelosaurine dinosaur from the Cenomanian-age Mussentuchit Member of the Cedar Mountain Formation, Utah. The Anatomical Record 307: 3717–3781. https://doi.org/10.1002/ar.25505

Barrett PM, Han F-L (2009) Cranial anatomy of *Jeholosaurus shangyuanensis* (Dinosauria: Ornithischia) from the Early Cretaceous of China. Zootaxa 2072: 31–55. https://doi.org/10.11646/zootaxa.2072.1.2

Barrett PM, Maidment SCR (2017) The evolution of ornithischian quadrupedality. Journal of Iberian Geology 43: 363–377. https://doi.org/10.1007/s41513-017-0036-0

Barta DE, Norell MA (2021) The Osteology of *Haya griva* (Dinosauria: Ornithischia) from the Late Cretaceous of Mongolia. Bulletin of the American Museum of Natural History 445: 1–112. https://doi.org/10.5531/sd.sp.47

Bertozzo F, Kecheng N, Gillette NV, Godefroit P (2025) Anatomical description and digital reconstruction of the skull of *Jeholosaurus shangyuanensis* (Dinosauria, Ornithopoda) from China. PLoS ONE 20: e0312519. https://doi.org/10.1371/journal.pone.0312519

Best LB, Gionfriddo JP (1991) Characterization of Grit Use by Cornfield Birds. The Wilson Bulletin 103: 68–82. https://doi.org/10.1007/978-1-4757-4901-4_3

Bonde JW, Hall RL, Krumenacker LJ, Varricchio DJ (2022) *Nevadadromeus schmitti* (gen. et sp. nov.), a New Basal Neornithischian with Affinities to the Thescelosaurinae, from the Upper Cretaceous (Cenomanian) Willow Tank Formation of Southern Nevada. Journal of the Arizona-Nevada Academy of Science 50: 1–8. https://doi.org/10.2181/036.050.0101

Boyd CA (2014) The cranial anatomy of the neornithischian dinosaur *Thescelosaurus neglectus*. PeerJ 2: e669. https://doi.org/10.7717/peerj.669

Boyd CA (2015) The systematic relationships and biogeographic history of ornithischian dinosaurs. PeerJ 3: e1523. https://doi.org/10.7717/peerj.1523

Brill K, Carpenter K (2001) A Baby Ornithopod from the Morrison Formation of Garden Park, Colorado. In: Tanke D, Carpenter K (Eds) Mesozoic Vertebrate Life. Indiana University Press, Bloomington, 197–205.

Brown CM, Boyd CA, Russell AP (2011) A new basal ornithopod dinosaur (Frenchman Formation, Saskatchewan, Canada), and implications for late Maastrichtian ornithischian diversity in North America. Zoological Journal of the Linnean Society 163: 1157–1198. https://doi.org/10.1111/j.1096-3642.2011.00735.x

Brown CM, Evans DC, Ryan MJ, Russell AP (2013) New data on the diversity and abundance of small-bodied ornithopods (Dinosauria, Ornithischia) from the Belly River Group (Campanian) of Alberta. Journal of Vertebrate Paleontology 33: 495–520. https://doi.org/10.1080/02724634.2013.746229

Butler RJ, Jin L, Chen J, Godefroit P (2011) The postcranial osteology and phylogenetic position of the small ornithischian dinosaur *Changchunsaurus parvus* from the Quantou Formation (Cretaceous: Aptian–Cenomanian) of Jilin Province, north-eastern China. Palaeontology 54: 667–683. https://doi.org/10.1111/j.1475-4983.2011.01046.x

Button DJ, Zanno LE (2023) Neuroanatomy of the late Cretaceous *Thescelosaurus neglectus* (Neornithischia: Thescelosauridae) reveals novel ecological specialisations within Dinosauria. Scientific Reports 13: 19224. https://doi.org/10.1038/s41598-023-45658-3

Campione NE, Evans DC, Brown CM, Carrano MT (2014) Body mass estimation in non-avian bipeds using a theoretical conversion to quadruped stylopodial proportions. Methods in Ecology and Evolution 5: 913–923. https://doi.org/10.1111/2041-210X.12226

Castanera D, Pascual C, Razzolini NL, Vila B, Barco JL, Canudo JI (2013) Discriminating between Medium-Sized Tridactyl Trackmakers: Tracking Ornithopod Tracks in the Base of the Cretaceous (Berriasian, Spain). PLoS ONE 8: e81830. https://doi.org/10.1371/journal.pone.0081830

Cerda IA (2008) Gastroliths in An Ornithopod Dinosaur. Acta Palaeontologica Polonica 53: 351–355. https://doi.org/10.4202/app.2008.0213

Chang KH, Seo SJ, Park SO (1982) Occurrence of a Dinosaur Limb Bone near Tabni, Southern Korea. Journal of Geological Society of Korea 18: 195–202. https://doi.org/10.14770/jgsk.1982.18.4.195

Chinzorig T, Takasaki R, Yoshida J, Tucker RT, Buyantegsh B, Mainbayar B, Tsogtbaatar K, Zanno LE (2025) A domed pachycephalosaur from the early Cretaceous of Mongolia. Nature 646(8087): 1138–1145. https://doi.org/10.1038/s41586-025-09213-6

Choi B-D, Jung J, Huh M (2023) Biostratigraphy and paleoecology of non-marine ostracods from the Cretaceous deposits in southwestern Korean Peninsula: a preliminary report. Journal of Geological Society of Korea 59: 495–511. https://doi.org/10.14770/jgsk.2023.030

Choi S, Lee Y-N (2017) A review of vertebrate body fossils from the Korean Peninsula and perspectives. Geosciences Journal 21: 867–889. https://doi.org/10.1007/s12303-017-0040-6

Chough SK, Sohn YK (2010) Tectonic and sedimentary evolution of a Cretaceous continental arc–backarc system in the Korean peninsula: New view. Earth-Science Reviews 101: 225–249. https://doi.org/10.1016/j.earscirev.2010.05.004

Cooper MR (1985) A revision of the ornithischian dinosaur *Kangnasaurus coetzeei* Haughton, with a classification of the Ornithischia. Annals of the South African Museum 95: 281–317. https://doi.org/10.5281/zenodo.16434376

Cruzado-Caballero P, Gasca JM, Filippi LS, Cerda IA, Garrido AC (2019) A new ornithopod dinosaur from the Santonian of Northern Patagonia (Rincón de los Sauces, Argentina). Cretaceous Research 98: 211–229. https://doi.org/10.1016/j.cretres.2019.02.014

Dong Z, Paik IS, Kim HJ (2001) A preliminary report on a sauropod from the Hasandong Formation (Lower Cretaceous), Korea. Proceedings of the Eighth Annual Meeting of the Chinese Society of Vertebrate Paleontology.

Fearon JL, Varricchio DJ (2015) Morphometric analysis of the forelimb and pectoral girdle of the Cretaceous ornithopod dinosaur *Oryctodromeus cubicularis* and implications for digging. Journal of Vertebrate Paleontology 35: e936555. https://doi.org/10.1080/02724634.2014.936555

Fonseca AO, Reid IJ, Venner A, Duncan RJ, Garcia MS, Müller RT (2024) A comprehensive phylogenetic analysis on early ornithischian evolution. Journal of Systematic Palaeontology 22: 2346577. https://doi.org/10.1080/14772019.2024.2346577

Galton PM (1974) The ornithischian dinosaur *Hypsilophodon* from the Wealden of the Isle of Wight. https://doi.org/10.5962/p.313819

Gierliński G, Karol S (2008) Stegosaurian footprints from the Morrison Formation of Utah and their implications for interpreting other ornithischian tracks. Oryctos 8: 29.

Gilmore CW (1915) Osteology of *Thescelosaurus*, an orthopodous dinosaur from the Lance Formation of Wyoming. Proceedings of the United States National Museum 49: 591–616. https://doi.org/10.5479/si.00963801.49-2127.591

Goloboff PA, Morales ME (2023) TNT version 1.6, with a graphical interface for MacOS and Linux, including new routines in parallel. Cladistics 39: 144–153. https://doi.org/10.1111/cla.12524

Griffin CT, Stocker MR, Colleary C, Stefanic CM, Lessner EJ, Riegler M, Formoso K, Koeller K, Nesbitt SJ (2021) Assessing ontogenetic maturity in extinct saurian reptiles. Biological Reviews 96: 470–525. https://doi.org/10.1111/brv.12666

Han F, Zhao Q, Stiegler J, Xu X (2020) Bone histology of the non-iguanodontian ornithopod *Jeholosaurus shangyuanensis* and its implications for dinosaur skeletochronology and development. Journal of Vertebrate Paleontology 40: e1768538. https://doi.org/10.1080/02724634.2020.1768538

Han F-L, Barrett PM, Butler RJ, Xu X (2012) Postcranial anatomy of *Jeholosaurus shangyuanensis* (Dinosauria, Ornithischia) from the Lower Cretaceous Yixian Formation of China. Journal of Vertebrate Paleontology 32: 1370–1395. https://doi.org/10.1080/02724634.2012.694385

Hone DWE, Farke AA, Wedel MJ (2016) Ontogeny and the fossil record: what, if anything, is an adult dinosaur? Biology Letters 12: 20150947. https://doi.org/10.1098/rsbl.2015.0947

Horner JR, De Ricqlès A, Padian K, Scheetz RD (2009) Comparative long bone histology and growth of the "hypsilophodontid" dinosaurs *Orodromeus makelai*, *Dryosaurus altus*, and *Tenontosaurus tillettii* (Ornithischia: Euornithopoda). Journal of Vertebrate Paleontology 29: 734–747. https://doi.org/10.1671/039.029.0312

Hu J, Xu X, Li F, Han F (2024) Tooth replacement in the early-diverging neornithischian *Jeholosaurus shangyuanensis* and implications for dental evolution and herbivorous adaptation in Ornithischia. BMC Ecology and Evolution 24: 46. https://doi.org/10.1186/s12862-024-02233-2

Hübner TR (2012) Bone Histology in *Dysalotosaurus lettowvorbecki* (Ornithischia: Iguanodontia) – Variation, Growth, and Implications. PLoS ONE 7: e29958. https://doi.org/10.1371/journal.pone.0029958

Hübner TR, Foth C, Heinrich W-D, Schwarz D, Bussert R (2021) Research history, taphonomy, and age structure of a mass accumulation of the ornithopod dinosaur *Dysalotosaurus lettowvorbecki* from the Upper Jurassic of Tanzania. Acta Palaeontologica Polonica 66: 275–300. https://doi.org/10.4202/app.00687.2019

Hübner TR, Rauhut OWM (2010) A juvenile skull of *Dysalotosaurus lettowvorbecki* (Ornithischia: Iguanodontia), and implications for cranial ontogeny, phylogeny, and taxonomy in ornithopod dinosaurs. Zoological Journal of the Linnean Society 160: 366–396. https://doi.org/10.1111/j.1096-3642.2010.00620.x

Huh M, Kim BS, Woo Y, Simon DJ, Paik IS, Kim HJ (2014) First record of a complete giant theropod egg clutch from Upper Cretaceous deposits, South Korea. Historical Biology 26: 218–228. https://doi.org/10.1080/08912963.2014.894998

Huh M, Lee D-G, Kim J-K, Lim J-D, Godefroit P (2011) A new basal ornithopod dinosaur from the Upper Cretaceous of South Korea. Neues Jahrbuch für Geologie und Paläontologie - Abhandlungen 259: 1–24. https://doi.org/10.1127/0077-7749/2010/0102

Huh M, Paik IS, Chung CH, Hwang KG, Kim BS (2003) Theropod tracks from Seoyuri in Hwasun, Jeollanamdo, Korea: occurrence and paleontological significance. Journal of the Geological Society of Korea 39: 461–478. https://doi.org/10.14770/jgsk.2003.39.4.461

Hwang K-G, Lockley MG, Huh M, Paik IS (2008) A reinterpretation of dinosaur footprints with internal ridges from the Upper Cretaceous Uhangri Formation, Korea. Palaeogeography, Palaeoclimatology, Palaeoecology 258: 59–70. https://doi.org/10.1016/j.palaeo.2007.10.029

Irmis RB (2007) Axial skeleton ontogeny in the Parasuchia (Archosauria: Pseudosuchia) and its implications for ontogenetic determination in archosaurs. Journal of Vertebrate Paleontology 27: 350–361. https://doi.org/10.1671/0272-4634(2007)27[350:ASOITP]2.0.CO;2

Jin L, Chen J, Zan S, Butler RJ, Godefroit P (2010) Cranial anatomy of the small ornithischian dinosaur *Changchunsaurus parvus* from the Quantou Formation (Cretaceous: Aptian–Cenomanian) of Jilin Province, northeastern China. Journal of Vertebrate Paleontology 30: 196–214. https://doi.org/10.1080/02724630903412372

Kim C-B, Kim J-M, Huh M (2008) Age and Stratification of Dinosaur Eggs and Clutches from Seonso Formation, South Korea. Journal of the Korean earth science society 29: 386–395. https://doi.org/10.5467/jkess.2008.29.5.386

Kim HM (1983) Cretaceous Dinosaurs from Korea. Journal of Geological Society of Korea 19: 115–126. https://doi.org/10.14770/jgsk.1983.19.3.115

Kim JK, Kwon YE, Lee SG, Lee JH, Kim JG, Huh M, Lee E, Kim YJ (2017) Disparities in correlating microstructural to nanostructural preservation of dinosaur femoral bones. Scientific Reports 7: 45562. https://doi.org/10.1038/srep45562

Kim JY, Huh M (2018) Dinosaurs, birds, and pterosaurs of Korea. Springer Singapore, 320 pp. https://doi.org/10.1007/978-981-10-6998-7_2

Kim KS, Lim JD, Lockley MG, Xing L, Kim DH, Piñuela L, Romilio A, Yoo JS, Kim JH, Ahn J (2018) Smallest known raptor tracks suggest microraptorine activity in lakeshore setting. Scientific Reports 8: 16908. https://doi.org/10.1038/s41598-018-35289-4

Kim KS, Lockley MG, Lim JD, Xing L (2019) Exquisitely-preserved, high-definition skin traces in diminutive theropod tracks from the Cretaceous of Korea. Scientific Reports 9: 2039. https://doi.org/10.1038/s41598-019-38633-4

Kim S, Hwang IG, Ghim YS, Kim N-H, Lee Y-N (2022) Upper Cretaceous (Coniacian-Santonian) dinosaur nesting colony preserved in abandoned crevasse splay deposits, Wi Island, South Korea. Palaeogeography, Palaeoclimatology, Palaeoecology 585: 110728. https://doi.org/10.1016/j.palaeo.2021.110728

Kim YH, Choi P-Y, Hwang JH, Kim HJ, Ko K, Chun HY (2014) Geological Report of the Mokpo Sheet (1:50,000). Korea Institute of Geoscience and Mineral Resources, Daejeon, 93 pp.

Kitchener JL, Campione NE, Smith ET, Bell PR (2019) High-latitude neonate and perinate ornithopods from the mid-Cretaceous of southeastern Australia. Scientific Reports 9: 19600. https://doi.org/10.1038/s41598-019-56069-8

Kraus MJ (1999) Paleosols in clastic sedimentary rocks: their geologic applications. Earth-Science Reviews 47: 41–70. https://doi.org/10.1016/S0012-8252(99)00026-4

Krumenacker L (2017) Osteology, phylogeny, taphonomy, and ontogenetic histology of *Oryctodromeus cubicularis*, from the Middle Cretaceous (Albian-Cenomanian) of Montana and Idaho. Montana State University, 267 pp.

Krumenacker LJ, Varricchio DJ, Organ C, Gardner JD, Britt BB, Boyd C (2023) Osteology and phylogenetic relationships of the mid-Cretaceous neornithischian dinosaur *Oryctodromeus cubicularis* Varricchio, 2007. Journal of Vertebrate Paleontology 43: e2330581. https://doi.org/10.1080/02724634.2024.2330581

Lee SY, Lee YN, Jung S-H (2024) A neornithischian phalanx from the Lower Cretaceous Tando beds of Ansan-si, Gyeonggi-do, South Korea. Journal of the Geological Society of Korea 60: 135–142. https://doi.org/10.14770/jgsk.2024.010

Lee Y-N, Yang SY (1997) Sauropod dinosaur remains from the Gyeongsang Supergroup, Korea. Paleontological Society of Korea Special Publication 2: 103–114.

Lee YN (2008) A dinosaur rib from the Gojeong-ri dinosaur egg site of Hwaseong City, Gyeonggi Province. Journal of the Paleontological Society of Korea 24: 127–133.

Lee YN, Ryan MJ, Kobayashi Y (2011) The first ceratopsian dinosaur from South Korea. Naturwissenschaften 98: 39–49. https://doi.org/10.1007/s00114-010-0739-y

Lewis PO (2001) A likelihood approach to estimating phylogeny from discrete morphological character data. Systematic Biology 50: 913–925. https://doi.org/10.1080/106351501753462876

Liang X, Wen S, Yang D, Zhou S, Wu S (2009) Dinosaur eggs and dinosaur egg-bearing deposits (Upper Cretaceous) of Henan Province, China: Occurrences, palaeoenvironments, taphonomy and preservation. Progress in Natural Science 19: 1587–1601. https://doi.org/10.1016/j.pnsc.2009.06.012

Liu S, Li Z, Liu D, O'Connor JK (2023) Quantifying the gastral mass in Early Cretaceous ornithuromorphs (Aves, Ornithothoraces) from the Jehol avifauna. Palaeontology 66: e12677. https://doi.org/10.1111/pala.12677

Lockley MG, Huh M, Kim BS (2012) *Ornithopodichnu*s and Pes-Only Sauropod Trackways from the Hwasun Tracksite, Cretaceous of Korea. Ichnos 19: 93–100. https://doi.org/10.1080/10420940.2011.625726

Madzia D, Boyd CA, Mazuch M (2018) A basal ornithopod dinosaur from the Cenomanian of the Czech Republic. Journal of Systematic Palaeontology 16: 967–979. https://doi.org/10.1080/14772019.2017.1371258

Maidment SCR, Barrett PM (2012) Does morphological convergence imply functional similarity? A test using the evolution of quadrupedalism in ornithischian dinosaurs. Proceedings of the Royal Society B: Biological Sciences 279: 3765–3771. https://doi.org/10.1098/rspb.2012.1040

Maidment SCR, Linton DH, Upchurch P, Barrett PM (2012) Limb-Bone Scaling Indicates Diverse Stance and Gait in Quadrupedal Ornithischian Dinosaurs. PLoS ONE 7: e36904. https://doi.org/10.1371/journal.pone.0036904

Makovicky PJ, Kilbourne BM, Sadleir RW, Norell MA (2011) A new basal ornithopod (Dinosauria, Ornithischia) from the Late Cretaceous of Mongolia. Journal of Vertebrate Paleontology 31: 626–640. https://doi.org/10.1080/02724634.2011.557114

Morris WJ (1976) Hypsilophodont dinosaurs: a new species and comments on their systematics. In: Churcher CS (Ed.) Essays on Palaeontology in Honour of Loris Shano Russell. Royal Ontario Museum, Toronto, 93–113. https://doi.org/10.5962/bhl.title.60760

Nogueira RA, Rozadilla S, Agnolín FL, Garcia Marsà JA, Motta MJ, Novas FE (2024) A new ornithopod from the Upper Cretaceous (Huincul Formation) of northwestern Patagonia, Argentina: Implications on elasmarian postcranial anatomy. Cretaceous Research 159: 105874. https://doi.org/10.1016/j.cretres.2024.105874

Norman DB (2004) Basal Iguanodontia. In: Weishampel DB, P. D, H O (Eds) The Dinosauria. University of California, Berkeley, 413–437. https://doi.org/10.1525/california/9780520242098.003.0022

Owen R (1842) Report on British fossil reptiles, part II. Report for the British Association for the Advancement of Science, Plymouth, 60–294.

Paik IS (2000) Bone chip-filled burrows associated with bored dinosaur bone in floodplain paleosols of the Cretaceous Hasandong Formation, Korea. Palaeogeography, Palaeoclimatology, Palaeoecology 157: 213–225. https://doi.org/10.1016/S0031-0182(99)00166-2

Paik IS, Huh M, Kim HJ (2004) Dinosaur egg-bearing deposits (Upper Cretaceous) of Boseong, Korea: occurrence, palaeoenvironments, taphonomy, and preservation. Palaeogeography, Palaeoclimatology, Palaeoecology 205: 155–168. https://doi.org/10.1016/j.palaeo.2003.12.007

Paik IS, Huh M, Park KH, Hwang KG, Kim KS, Kim HJ (2006) Yeosu dinosaur track sites of Korea: The youngest dinosaur track records in Asia. Journal of Asian Earth Sciences 28: 457–468. https://doi.org/10.1016/j.jseaes.2005.11.007

Park JY (2016) Comments on the validity of the taxonomic status of "*Pukyongosaurus*"(Dinosauria: Sauropoda). Memoir of the Fukui Prefectural Dinosaur Museum 15: 27–32.

Park K-H (2012) Cyclic igneous activities during the Late Paleozoic to Early Cenozoic period over the Korean peninsula. The Journal of the Petrological Society of Korea 21: 193–202. https://doi.org/10.7854/jpsk.2012.21.2.193

Pintore R, Houssaye A, Hutchinson JR (2025) How femoral morphology informs our understanding of the evolution of ornithopod locomotion and body size. Palaeontology 68: e70016. https://doi.org/10.1111/pala.70016

Poole K (2023) Placing juvenile specimens in phylogenies: An ontogenetically sensitive phylogenetic assessment of a new genus of iguanodontian dinosaur from the Early Cretaceous Kirkwood Formation, South Africa. The Anatomical Record 306: 1939–1950. https://doi.org/10.1002/ar.25095

Rhee C-Y, Kim B-S, Kim M-G, Kim C-B (2012) K-Ar Ages of Dinosaur Egg Nest found in Cretaceous Formation of Aphaedo, Jeollanam-do, Korea. Journal of the Korean earth science society 33: 329–336. https://doi.org/10.5467/jkess.2012.33.4.329

Ronquist F, Teslenko M, Van Der Mark P, Ayres DL, Darling A, Höhna S, Larget B, Liu L, Suchard MA, Huelsenbeck JP (2012) MrBayes 3.2: efficient Bayesian phylogenetic inference and model choice across a large model space. Systematic biology 61: 539–542. https://doi.org/10.1093/sysbio/sys029

Sagong H, Kwon S-T, Ree J-H (2005) Mesozoic episodic magmatism in South Korea and its tectonic implication. Tectonics 24: TC5002. https://doi.org/10.1029/2004TC001720

Scheetz RD (1999) Osteology of *Orodromeus makelai* and the phylogeny of basal ornithopod dinosaurs. Montana State University, 186 pp.

Scotese CR (2021) An Atlas of Phanerozoic Paleogeographic Maps: The Seas Come In and the Seas Go Out. Annual Reviews of Earth and Planetary Sciences 49: 679–728. https://doi.org/10.1146/annurev-earth-081320-064052

Seeley HG (1887) On the classification of the fossil animals commonly named Dinosauria. Proceedings of the Royal Society of London 43: 165–171. https://doi.org/10.1098/rspl.1887.0117

Simon DJ, Varricchio DJ, Jin X, Robison SF (2018) Microstructural overlap of *Macroelongatoolithus* eggs from Asia and North America expands the occurrence of colossal oviraptorosaurs. Journal of Vertebrate Paleontology 38: e1553046. https://doi.org/10.1080/02724634.2018.1553046

Snyder K, McLain M, Wood J, Chadwick A (2020) Over 13,000 elements from a single bonebed help elucidate disarticulation and transport of an *Edmontosaurus thanatocoenosis*. PLoS ONE 15: e0233182. https://doi.org/10.1371/journal.pone.0233182

Sternberg C (1937) A classification of *Thescelosaurus*, with a description of a new species. Proceedings of the Geological Society of America 1936: 375.

Sues H-D (1980) Anatomy and relationships of a new hysilophodontid dinosaur from the Lower Cretaceous of North America. Palaeontographica Abt A 169: 51–72.

Sues H-D, Evans DC, Galton PM, Brown CM (2023) Anatomy of the neornithischian dinosaur *Parksosaurus warreni* (Parks, 1926) from the Upper Cretaceous (lower Maastrichtian) Horseshoe Canyon Formation of Alberta, Canada. Cretaceous Research 141: 105369. https://doi.org/10.1016/j.cretres.2022.105369

Takasaki R (2020) Herbivorous adaptations of Dinosauria: hadrosaurid foraging strategy and archosaur gastroliths. Hokkaido University, 300 pp.

Takasaki R, Kobayashi Y (2024) Anatomical description of neornithine stomach with implications on neornithine stomach morphology. Journal of anatomy 245: 787–796. https://doi.org/10.1111/joa.14123

Varricchio DJ, Martin AJ, Katsura Y (2007) First trace and body fossil evidence of a burrowing, denning dinosaur. Proceedings of the Royal Society B: Biological Sciences 274: 1361–1368. https://doi.org/10.1098/rspb.2006.0443

Weishampel DB, Jianu CM, Csiki Z, Norman DB (2003) Osteology and phylogeny of *Zalmoxes* (n. g.), an unusual Euornithopod dinosaur from the latest Cretaceous of Romania. Journal of Systematic Palaeontology 1: 65–123. https://doi.org/10.1017/S1477201903001032

Wings O (2004) Identification, distribution, and function of gastroliths in dinosaurs and extant birds with emphasis on ostriches (*Struthio camelus*). Universität Bonn, 189 pp.

Wings O, Sander PM (2007) No gastric mill in sauropod dinosaurs: new evidence from analysis of gastrolith mass and function in ostriches. Proceedings of the Royal Society B: Biological Sciences 274: 635–640. https://doi.org/10.1098/rspb.2006.3763

Yang Y, Wu W, Dieudonné P-E, Godefroit P (2020) A new basal ornithopod dinosaur from the Lower Cretaceous of China. PeerJ 8: e9832. https://doi.org/10.7717/peerj.9832

Yoon HS, Kim HW, Park J-Y, Jung S-H, Kong D-Y, Lee Y-N (2026) First reports of a probable ankylosaurian (Thyreophora) trackway from the Jindong Formation (Cenomanian) of Goseong County, South Korea. Cretaceous Research 178: 106240. https://doi.org/10.1016/j.cretres.2025.106240

Yoon HS, Lee Y-N, Jung S-H, Kong D-Y, Kim S-H, Son M (2021) A juvenile ornithopod tracksite from the Lower Cretaceous Haman Formation, South Korea. Cretaceous Research 125: 104877. https://doi.org/10.1016/j.cretres.2021.104877

Supplementary material 1

Phylogenetic results and histological images

Authors: Jongyun Jung, Minguk Kim, Hyemin Jo, Julia A. Clarke
Data type: docx

Link: https://doi.org/10.3897/fr.29.178152.suppl1

Supplementary material 2

Character matrix

Authors: Jongyun Jung, Minguk Kim, Hyemin Jo, Julia A. Clarke
Data type: xlsx

Link: https://doi.org/10.3897/fr.29.178152.suppl2

Supplementary material 3

Gastrolith dataset

Authors: Jongyun Jung, Minguk Kim, Hyemin Jo, Julia A. Clarke
Data type: xlsx
Explanation note: Gastrolith dataset for gastrolith and body mass correlations

Link: https://doi.org/10.3897/fr.29.178152.suppl3

Supplementary material 4

TNT script file for parsimony analyses using the matrix of Fonseca et al. (2024)

Authors: Jongyun Jung, Minguk Kim, Hyemin Jo, Julia A. Clarke
Data type: tnt

Link: https://doi.org/10.3897/fr.29.178152.suppl4

Supplementary material 5

NEXUS script file for the tip-dated Bayesian analyses using the matrix of Fonseca et al. (2024)

Authors: Jongyun Jung, Minguk Kim, Hyemin Jo, Julia A. Clarke
Data type: nex

Link: https://doi.org/10.3897/fr.29.178152.suppl5

Supplementary material 6

TNT script file for parsimony analyses using the matrix of Avrahami et al. (2024)

Authors: Jongyun Jung, Minguk Kim, Hyemin Jo, Julia A. Clarke
Data type: tnt

Link: https://doi.org/10.3897/fr.29.178152.suppl6

Supplementary material 7

NEXUS script file for the tip-dated Bayesian analyses using the matrix of Avrahami et al. (2024)

Authors: Jongyun Jung, Minguk Kim, Hyemin Jo, Julia A. Clarke
Data type: nex

Link: https://doi.org/10.3897/fr.29.178152.suppl7